Identification de nouveaux immunomarqueurs du rejet humoral actif en transplantation rénale à travers l'analyse du protéome glomérulaire par spectrométrie de masse

Bertrand Chauveau

université de BORDEAUX

U.F.R. DES SCIENCES MEDICALES

Année 2020 Thèse n°3112

THESE POUR L'OBTENTION DU

DIPLOME D'ETAT de DOCTEUR EN MEDECINE

Présentée et soutenue publiquement

Par CHAUVEAU Bertrand Camille Geoffroy

Né le 17 Février 1990 à Suresnes

Le vendredi 2 Octobre 2020

IDENTIFICATION DE NOUVEAUX IMMUNOMARQUEURS DU REJET HUMORAL ACTIF EN TRANSPLANTATION RENALE A TRAVERS L'ANALYSE DU PROTEOME GLOMERULAIRE PAR SPECTROMETRIE DE MASSE

Sous la direction du Professeur Pierre MERVILLE

Membres du jury :

Madame le Professeur Béatrice VERGIER	Président
Madame le Docteur Marion RABANT	Rapporteur
Madame le Professeur Brigitte LE BAIL	Examinateur
Monsieur le Professeur Christian COMBE	Examinateur
Monsieur le Professeur Pierre DUBUS	Examinateur
Monsieur le Professeur Pierre MERVILLE	Directeur

REMERCIEMENTS

A mon maitre et Président de jury de thèse

Madame le Professeur Béatrice VERGIER

Vous me faîtes l'honneur de présider ce jury.

Je vous remercie vivement pour tout ce que vous avez pu m'apporter et de votre soutien au projet hospitalo-universitaire que je porte. Votre énergie, votre enthousiasme et votre dévouement au quotidien est un exemple pour nous tous.

A mon jury de thèse

Madame le Professeur Brigitte LE BAIL

Vous me faîtes l'honneur de juger ce travail. Toujours un plaisir de travailler avec vous, tant sur le plan sanitaire que sur les projets de recherche et développement. Hâte que ces derniers avancent.

Madame le Docteur Marion RABANT

Tu me fais l'honneur de juger ce travail et c'est un grand plaisir pour moi de t'avoir dans ce jury. Je te suis extrêmement reconnaissant de m'avoir formé, avec Jean-Paul, à cette belle discipline qu'est la Néphropathologie, au cours d'un semestre grâce à toi très sympathique et enrichissant.

Monsieur le Professeur Christian COMBE

Vous me faîtes l'honneur de juger ce travail. Je vous suis très reconnaissant de ce que vous m'avez apporté ainsi que de votre sympathie à mon égard. Souvenir d'un stage clinique très enrichissant. Il vous faudra malheureusement encore supporter une soutenance de thèse dans le domaine de la transplantation, et un candidat sans cravate…

Monsieur le Professeur et Doyen de notre faculté Pierre DUBUS

Vous me faîtes l'honneur de juger ce travail. Je vous suis extrêmement reconnaissant du soutien que vous portez à mon projet hospitalo-universitaire. Souvenir de votre grande pédagogie autour de quelques clonalités…

Monsieur le Professeur et Vice-Doyen de notre faculté Pierre MERVILLE

Vous m'avez fait l'honneur de diriger ce travail. Je ne vous remercierai jamais assez de votre soutien, de votre implication majeure dans l'encadrement de ce travail de thèse et plus généralement dans mon cursus universitaire. Travailler avec vous est très enrichissant et j'espère que l'avenir sera concluant.

Remerciements personnels

A mes parents, à qui je dois beaucoup, si ce n'est tout. Merci de m'avoir soutenu dans ce que j'ai pu entreprendre et de me soutenir encore aujourd'hui. Vous comptez pour moi plus que je ne saurais le dire.

A mon frère Benoît. Merci d'être tout simplement et merveilleusement qui tu es. Tu as toujours été pour moi une référence. Merci de répondre présent lorsque j'ai en ai besoin.

A ma nièce, Céleste, qui grandit déjà si vite (1 an déjà). Tu ne liras probablement jamais ceci, mais qu'importe.

A mes grands-parents, mamie Jeanine et grand-père Gérard, vous ne pouvez être présents ce jour, mais je sais que le cœur y est. Mamie Thérèse et grand-père Guy, vous n'êtes plus là mais je pense à vous.

A ma tante Nathalie et mes cousins Julien et Justine, on ne se voit pas souvent ce qui ne m'empêche pas de bien penser à vous.

A mon oncle et parrain Pascal. Toujours agréable de discuter avec quelqu'un d'aussi cultivé que toi. Souvenir d'une balade dans le parc Montsouris.

A ma marraine, Agnès. Toujours un plaisir de te voir. Une bonne raison de plus pour aller en Suisse.

A ma belle-sœur Pauline, qui fait des efforts pour me supporter. Je n'oublie pas le reste de la famille Malhanche, Sylvie, Gabriel et mémé Jeannette.

A Etienne, pour son inoxydable amitié. J'ai toujours pu compter sur toi, merci. A quand le prochain nouvel an au château ?

A Thibault et tous ces bons moments passés ensemble, notamment à travers l'école de golf (« quel talent ! »), ces vacances à Royan en MG… Merci de me supporter comme je suis, et notamment ma vision très personnelle des conversations par textos (nan mais je progresse, c'est évident. Comment ça, une photo ?). Je n'oublie pas Manon évidemment. Fier de pouvoir être votre témoin, trop hâte !

A Sylvain, pour ses leçons qu'il nous met tous à Mario Kart (sans parler de Smash Bros), ce fameux demi-cochon qu'on a coupé ensemble. Je n'oublie pas Caterin, et bien sûr la petite Juliette.

A Alexis, toujours de bonne compagnie, même si on ne s'entendra jamais au sujet des grèves de la SNCF…

A Jean, Félix et Nicolas, pour ces belles années à Clermont-Ferrand, et ce soutien mutuel pour l'ECN. Dommage que nos occupations respectives nous aient séparé autant, mais promis on se va se faire un truc. Bien sûr une pensée pour Marine et Laurine.

A Julien, digne disciple de Frantz. Toujours espiègle, souvent caustique, parfois acerbe, toujours marrant.

A tous mes co-internes d'anapath que cette période m'a permis de rencontrer : Aude et sa bonne humeur (parfois déplacée), Julie et ses graines de chia (euh…), Chloé D., Mégane, Yara, Hugo, mais aussi Sandra, Mégane, Rémi, Côme, Julia, Damien, Camille, Chloé C., Marie, Paul, Anaïs, Léonie, Lucile, Mathieu et Laure-Amandine

Aux anciens co-internes devenus grands : Sarah, Fanny, Adeline, Clémence, Camille, Elodie, Frantz et bien sûr Benjamin

A la team des radio golfeurs : François pour m'avoir appris tout ce que je sais de l'échographie abdominale et ses « conseils » avisés aux urgences, Alexis (à quand une revanche ?)

A Cécile et Cyril, les compères du DIU Néphropath

A Pierre, Frédéric et Sophie, pour cette bonne ambiance et m'avoir soutenu pendant ce passage somme toute complexe en Néphrologie. Best co-internes ever++, un câlin ?

A Agathe, pour ces belles années à venir (enfin on l'espère)

A Jean-Paul et Marion, pour ce super semestre passé à Necker, et m'avoir appris tout ce que je sais de la Néphropathologie, dans la bonne ambiance. Toujours un plaisir de travailler avec vous.

Un grand merci à Jonathan, toujours hyper réactif pour une relecture ou dès qu'une question se pose en Immunologie.

A Hannah, pour ces relectures attentives et ses bonnes idées.

Aux différentes équipes médicales et paramédicales qui m'ont accueilli au cours de mon internat :

Merci à toute l'équipe du service de Néphrologie-Transplantation de Pellegrin pour m'avoir encadré quand j'étais perdu en clinique : Benjamin, Emma, Mathilde, Charlotte, Sébastien, Karine, … Mentions spéciales à Lionel pour ses relectures attentives et ses conseils avisés et à Claire pour son implication et son soutien.

Merci à toute l'équipe d'anapath du CH de Pau (Valérie, Sophie et Martie), pour ce stage qui m'a conforté dans ce choix de spécialité.

Merci à toute l'équipe d'anapath de Haut-Lévêque (Marion, Hélène, Geneviève, Hugues, Marie P, Marie J, Annick et Marie-Laure) et mais aussi celle du SBT (Pr Merlio, Audrey, Charline et David).

Merci à toute l'équipe d'anapath de Bergonié (Gaëtan, Houda, Sabrina, Benjamin, Florence). Mentions spéciales au Pr Coindre pour ces cours de tissus mous empreints de passion, et à François, notre coordonnateur, toujours disponible et à l'écoute quand un problème se pose.

Merci à toute l'équipe d'anapath de Pellegrin (Guillaume, Skander, Raul, Anne, Mokrane, Marie-Laure, Sandrine et bien sûr les foetopath). Mention spéciale pour Claire, qui supporte mes accès de désespoir ou de ronchonnements.

Merci à toute l'équipe du laboratoire U1053 et son étage, notamment à Frédéric, Anne-Aurélie, Sylvaine, Cyril, Nathalie et Virginie.

Enfin, à Sébastien Lepreux et au Professeur Anne Vital, pour m'avoir mis sur la voie de la néphropathologie

« L'œil écoute ». L'œil scrute, fouille, décrit mais aussi écrit. […] Le pathologiste a non seulement la faculté que possède l'esprit de se représenter des images, mais aussi la capacité de les interpréter, d'en reconstituer l'histoire, de créer des liens entre les images.

Jean-Pierre Grünfeld
Préface de l'Atlas de Pathologie rénale, Laure-Hélène Noël
Flammarion Médecine-Sciences, 2008

A mes grands-parents,

A mes parents,

A mon frère,

A ma nièce,

Table des matières

Liste des abréviations utilisées

(par ordre alphabétique)

aABMR : *active antibody-mediated rejection* ou rejet humoral actif

ACN : acétonitrile

ASS1 : ArgininoSuccinate Synthase 1

B-HOT *: Banff-Human Organ Transplant*

caABMR : *chronic active antibody-mediated rejection* ou rejet humoral chronique actif

CTL : *cytotoxic T lymphocytes* ou lymphocytes T cytotoxiques

cg : *transplant glomerulopathy* ou glomérulopathie d'allogreffe

CORO1A : *coronin-1A*

cpt : *peritubular capillaritis* ou capillarite péritubulaire

DFG : débit de filtration glomérulaire

DNAJB9 : *DnaJ Homolog Subfamily B Member 9*

DSA : *Donor-Specific Antibodies* ou anticorps spécifiques du donneur

EIF2 : *Eukaryotic translation Initiation Factor 2*

FFPE : *Formalin-Fixed and Paraffin-Embedded* ou fixé en formol et inclus en paraffine

g : *glomerulitis* ou glomérulite

GBP1 : *guanylate-binding protein 1*

HLA : *Human Leukocyte Antigens* ou antigènes leucocytaires humains

IFN-γ : interféron-γ

IF/TA : *Interstitial Fibrosis and Tubular Atrophy* ou fibrose interstitielle et atrophie tubulaire

IVIG : *intravenous immunoglobulins* ou immunoglobulines intraveineuses

IQR : intervalle interquartile

IRCT : insuffisance rénale chronique terminale

LC-MS/MS : chromatographie en phase liquide couplée à la spectrométrie de masse en tandem

MAC : *membrane attack complex* ou complexe d'attaque membranaire

MEC : matrice extracellulaire

MFI : *Mean Fluorescence Intensity* ou intensité moyenne de fluorescence

MVI : *Microvascular Inflammation* ou inflammation de la microcirculation

NK : *Natural Killer*

PEN : polyéthylène naphthalate

PKR : *double stranded RNA-dependent protein kinase*

SDS-PAGE : électrophorèse sur gel de polyacrylamide contenant du dodécylsulfate de sodium

SG : *stable graft* ou greffé stable

TYMP : *thymidine phosphorylase*

WARS : *tryptophan--tRNA ligase, cytoplasmic*

I- Introduction

A) Place du rejet humoral en transplantation rénale

La transplantation rénale représente le traitement de choix de l'insuffisance rénale chronique terminale, permettant une meilleure survie des patients comparativement à la dialyse tout en améliorant leur qualité de vie. En France, environ 3 600 patients ont bénéficié d'une transplantation rénale sur l'année 2018, pour un total de 41 000 patients transplantés rénaux et porteurs d'un greffon fonctionnel (1). Malgré ces chiffres, le nombre de patients en attente d'une greffe rénale s'accroît, estimé à 15 000 patients au 1er janvier 2019. Dans ce contexte, atteindre une survie optimale des greffons fonctionnels est un objectif fondamental.

La perte de greffon est un processus éminemment multifactoriel (2), mais qui fait intervenir en premier lieu les mécanismes immuns de rejet d'allogreffe, en lien essentiellement avec les incompatibilités donneur/receveur dans le système des antigènes leucocytaires humains (*Human Leukocyte Antigens* ou HLA). Le rejet d'allogreffe est conceptuellement séparé en deux grandes entités : rejet cellulaire médié par les lymphocytes T du receveur et rejet humoral médié par des anticorps produits par le receveur et dirigés contre des antigènes du donneur (*donor-specific antibodies* ou DSA). Comme l'illustre la Figure 1*, l'apparition de nouvelles molécules immunosuppressives au cours des dernières décennies a permis une spectaculaire réduction de l'incidence du rejet aigu au cours de la première année de greffe, qui s'est traduite par une amélioration de la survie à court terme des greffons rénaux.

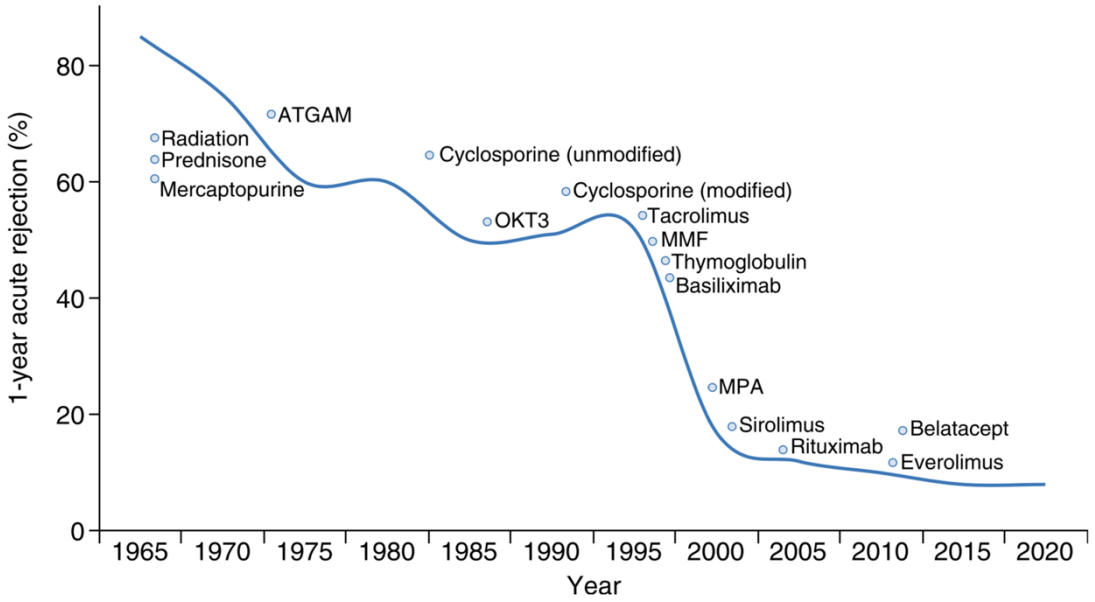

Figure 1* : Déclin de l'incidence du rejet aigu à 1 an de transplantation au cours du temps avec date approximative de l'introduction des traitements immunosuppresseurs

d'après Cooper, 2020 (3)

Malheureusement, cette avancée importante ne s'est pas traduite par une progression de la survie à long terme, au contraire (4). Ainsi, selon les dernières données du rapport de l'Agence de biomédecine 2018, la comparaison de la survie des greffons après transplantation rénale (Figure 2*) montre une baisse modeste mais significative de la survie à 5 ans, passant de 80,1% à 77,9% entre les périodes 2006-2008 et 2012-2014 (1).

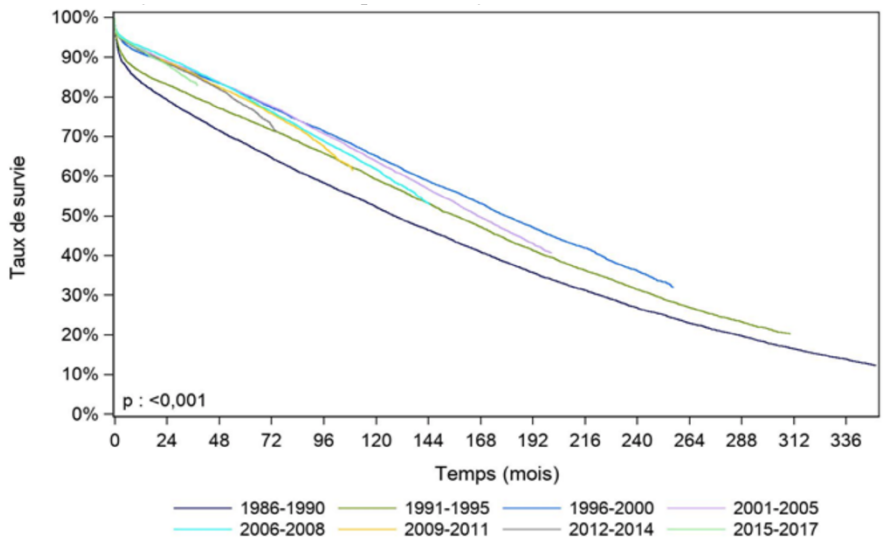

Figure 2* : Survie du greffon rénal selon la période de greffe

d'après le rapport Médical et Scientifique 2018, Agence de Biomédecine (1)

Un responsable majeur de la perte du greffon en transplantation rénale est le rejet humoral, actuellement reconnu comme le principal facteur de perte du greffon sur le long terme (2). Ainsi sur une série canadienne de 315 patients porteurs d'une greffon rénal et biopsiés sur indication, près de 65% des dysfonctions ou pertes de greffon étaient imputables au rejet humoral ou mixte (2). Une étude belge portée par Naesens *et al.* et intéressant 1 197 patients greffés rénaux avec un suivi moyen de 14 ans après leur transplantation, montrait que sur les 144 patients ayant perdu leur greffon, près de 40% d'entre eux présentaient des lésions histologiques suggestives de rejet humoral sur leur dernière biopsie pour indication (5). La Figure 3* illustre à la fois la forte prévalence du rejet humoral chronique (glomérulopathie d'allogreffe) dans la pathologie du greffon rénal sur le long terme mais aussi le caractère éminemment multifactoriel des lésions pouvant être retrouvées après quelques mois de greffe, une cause unique de perte de greffon pouvant être identifiée dans moins de 7 % des cas.

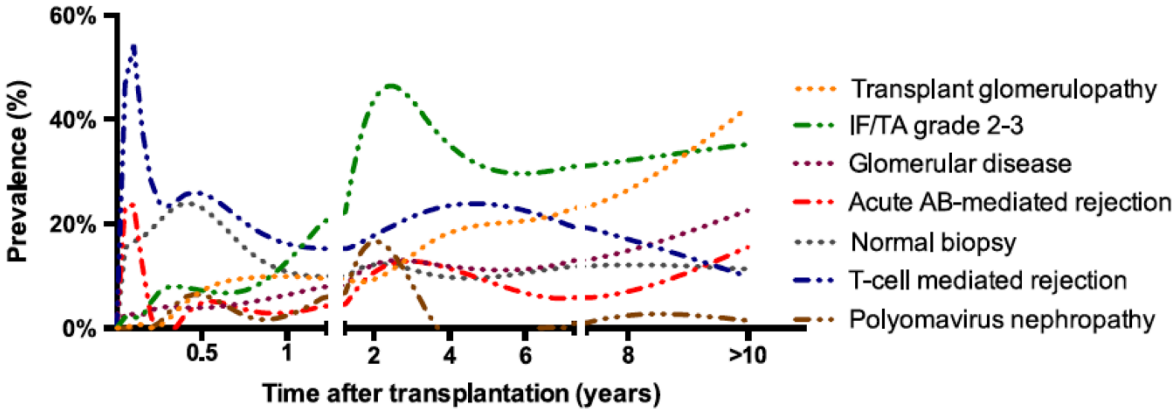

Figure 3* : Prévalence au cours du temps après transplantation des atteintes histologiques du greffon, d'après Naesens *et al.* (5)

IF/TA : *Interstitial Fibrosis and Tubular Atrophy* ou fibrose interstitielle et atrophie tubulaire

AB : *antibody-mediated* ou médiés par anticorps

Dans les années 2000, l'incidence du rejet humoral aigu en transplantation rénale était évaluée à près de 7% des cas (6). Mais l'évolution de la définition du rejet humoral au fil des années, et notamment la reconnaissance du rejet humoral C4d négatif depuis 2013, a majoré son incidence de l'ordre de 50 à 100% chez les patients présentant des DSA sériques (7). L'incidence du rejet humoral aigu varie également en fonction du risque immunologique, compliquant entre 20 et 50% des greffes à haut risque dites HLA-incompatibles (greffe en présence de DSA) (8). Quant à la glomérulopathie d'allogreffe (cg), très associée au rejet humoral chronique, sa fréquence est évaluée aux alentours de 20% à 5 ans (9).

Comme le résume la Figure 4*, la stratégie thérapeutique actuelle du rejet humoral actif en transplantation rénale repose sur une combinaison de modalités ayant pour buts d'épurer ou de moduler les DSA circulants, de limiter leurs effets et/ou de limiter leur production. Les échanges plasmatiques et/ou les perfusions intraveineuses d'immunoglobulines polyvalentes associés à l'adjonction de glucocorticoïdes restent les piliers du traitement (4). Malgré une efficacité à long terme souvent décevante sur la survie du greffon, ces protocoles thérapeutiques sont à risque d'effets secondaires non négligeables (infectieux notamment), nécessitant donc des indications précises, et une définition rigoureuse du rejet humoral.

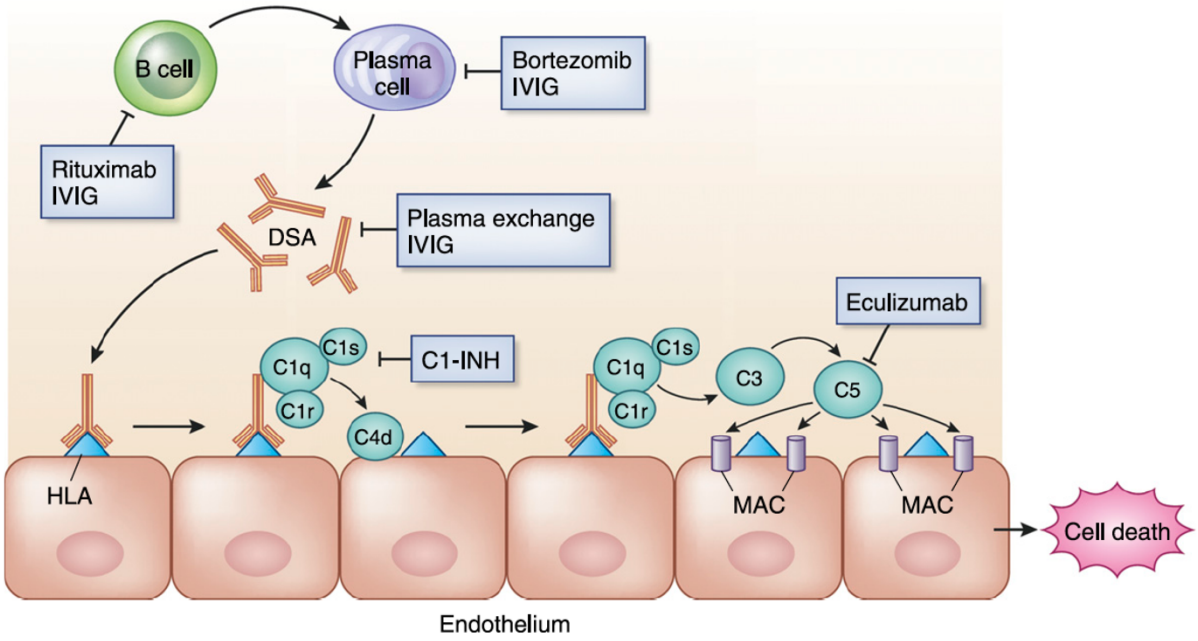

Figure 4* : Cibles des thérapies disponibles ou expérimentales pour le rejet humoral actif

d'après Cooper, 2020 (3)

HLA : *Human Leukocyte Antigens* ou antigènes leucocytaires humains ; INH : inhibiteur ;

IVIG : intravenous immunoglobulins ou immunoglobulines intraveineuses *; MAC : membrane attack complex* ou complexe d'attaque membranaire

B) Physiopathologie et phénotypes du rejet humoral en transplantation rénale

Le rejet humoral est conceptuellement médié par des anticorps, produits par le receveur, et dirigés contre des antigènes du greffon rénal, définis comme anticorps spécifiques du donneur (DSA). Ceux-ci peuvent reconnaître le système HLA du donneur, mais également des antigènes endothéliaux ou des antigènes de groupe sanguin en cas de greffe ABO-incompatible (10). On distingue ainsi des rejets humoraux avec DSA anti-HLA, de rejets humoraux avec DSA non anti-HLA. Les DSA peuvent être préexistants à la greffe en cas d'événement(s) immunisant(s) antérieur(s), ou apparaître *de novo* au décours de la transplantation. Leur présence dans le sérum du receveur est associée à une moindre survie du greffon (11). La fixation des DSA et leur interaction avec les cellules endothéliales du greffon représentent le *primum movens* de leur cascade pathogénique. Leur capacité à recruter les protéines du complément par la voie classique entraine son activation et lèse les cellules endothéliales, *via* la liaison covalente d'une fraction de la protéine du complément C4, le C4b, qui sera finalement dégradé en C4d, critère diagnostique clef du rejet humoral depuis 2001 (12,13). L'activation du complément participe ainsi au recrutement d'effecteurs inflammatoires, notamment au moyen des anaphylatoxines C3a et C5a (14). D'autres mécanismes pro-inflammatoires sont également impliqués au cours du rejet humoral, notamment de cytotoxicité dépendante des anticorps médiée par les cellules NK et les

monocytes/macrophages *via* leurs récepteurs au fragment Fc des immunoglobulines (15). Ces mécanismes participent ainsi au recrutement et à l'activation de cellules immunitaires au niveau de la microcirculation, dénommés inflammation de la microcirculation (MVI), déterminant essentiel du rejet humoral sur le plan histologique. La figure 5* illustre les principaux mécanismes physiopathologiques du rejet humoral. Enfin, de récents travaux ont révélé l'existence de rejets vasculaires, apparaissant purement médiés par les cellules *Natural Killer* (NK), avec une pathogénicité indépendante des DSA. Dans ce cadre, les disparités génétiques entre donneur et receveur dans les molécules HLA de classe I, détectées par les cellules NK à la surface des cellules endothéliales du greffon, entrainent leur activation et des lésions *in fine* de MVI, dans une situation de « pseudo *missing-self* » (16). Cette forme de rejet microvasculaire s'accompagne des mêmes lésions histologiques de MVI que le rejet humoral.

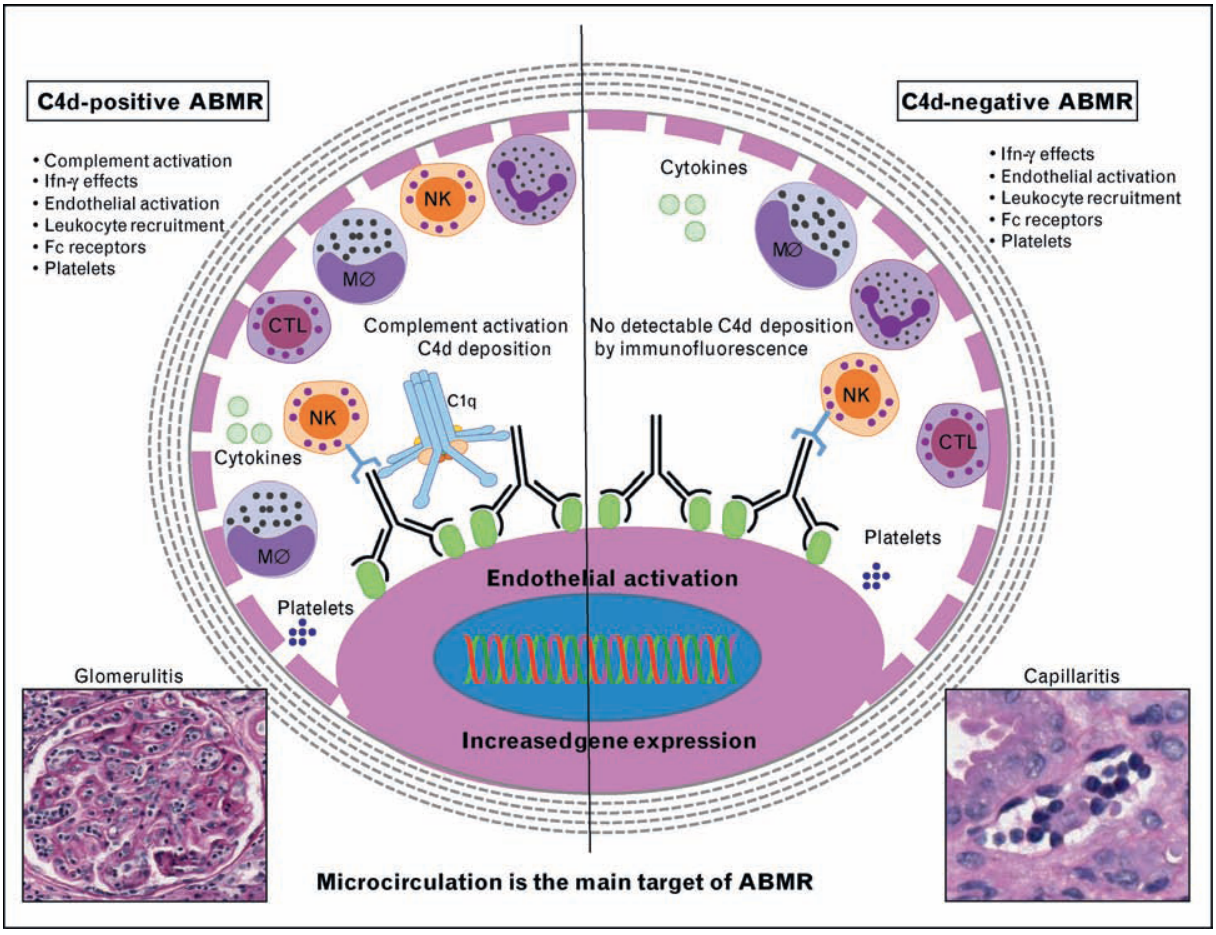

Figure 5* : Représentation schématique des principaux mécanismes moléculaires impliqués au cours du rejet humoral, d'après Sis et Halloran (17)

ABMR : *antibody-mediated rejection* ou rejet humoral ; CTL : lymphocytes T cytotoxiques

Mø : monocytes–macrophages ; IFN-γ : interféron gamma ; NK : natural killer

C) Définition du rejet humoral en transplantation rénale

Sa définition est établie par la classification internationale de Banff, actualisée tous les deux ans depuis 1991, la dernière datant de 2019 (18). Cette classification se base sur différentes lésions élémentaires, dont l'intensité est gradée de 0 à 3. Concernant le rejet humoral, deux versants sont distingués : rejet humoral actif et chronique actif.

a- Rejet humoral actif

Le terme de rejet humoral actif nécessite une combinaison de trois critères, histopathologiques et biologique :

- 1 : Preuve histologique d'une agression tissulaire aigue, caractérisée par un ou plusieurs des critères suivants :
  - ⇨ Inflammation de la microcirculation (glomérulite g > 0 et/ou capillarite péritubulaire cpt > 0), en l'absence d'une glomérulopathie récidivante ou *de novo*. En présence d'un rejet cellulaire aigu, d'un infiltrat *borderline* ou d'une infection, un score cpt > 0 seul est insuffisant et g doit être > 0.
  - ⇨ Artérite intimale ou transmurale (v > 0)
  - ⇨ Microangiopathie thrombotique, en l'absence d'autre cause
  - ⇨ Nécrose tubulaire aigue, en l'absence d'autre cause

- 2 : Preuve histologique d'une interaction récente/en cours des anticorps du patient avec l'endothélium du greffon, caractérisée par un ou plusieurs des critères suivants :
  - ⇨ Marquage linéaire du C4d sur les capillaires péritubulaires ou les *vasa recta* médullaires, évalué en immunofluorescence ou immunohistochimie par révélation enzymatique
  - ⇨ Inflammation de la microcirculation au minimum modérée, définie par la somme g + cpt ≥ 2, en l'absence d'une glomérulopathie récidivante ou *de novo*. En présence d'un rejet cellulaire aigu, d'un infiltrat *borderline* ou d'une infection, un score cpt > 0 seul est insuffisant et g doit être > 0.
  - ⇨ Expression accrue de transcrits de gènes/classificateurs sur biopsie fortement associés au rejet humoral, si clairement validés

- 3 : Présence de DSA circulants dans le sérum du patient, critère dont la présence n'est plus obligatoire depuis l'actualisation de la classification de Banff 2017. En effet, les dépôts de C4d ou bien les classificateurs moléculaires peuvent se substituer à la positivité des DSA.

b- Rejet humoral chronique actif

Il est défini par la conjonction des critères suivants :

- 1 : Preuve histologique d'une agression tissulaire chronique : glomérulopathie d'allogreffe (cg : aspect de doubles contours de la membrane basale glomérulaire) en l'absence d'une microangiopathie thrombotique ou d'une glomérulopathie récidivante ou *de novo* ; ou bien un aspect feuilleté de la membrane basale des capillaires péritubulaires (uniquement visible en microscopie électronique) ou encore la présence d'une fibrose intimale artérielle récente sans autre cause évidente.
- 2 et 3 : similaires à ceux du rejet humoral actif tel que décrit ci-dessus.

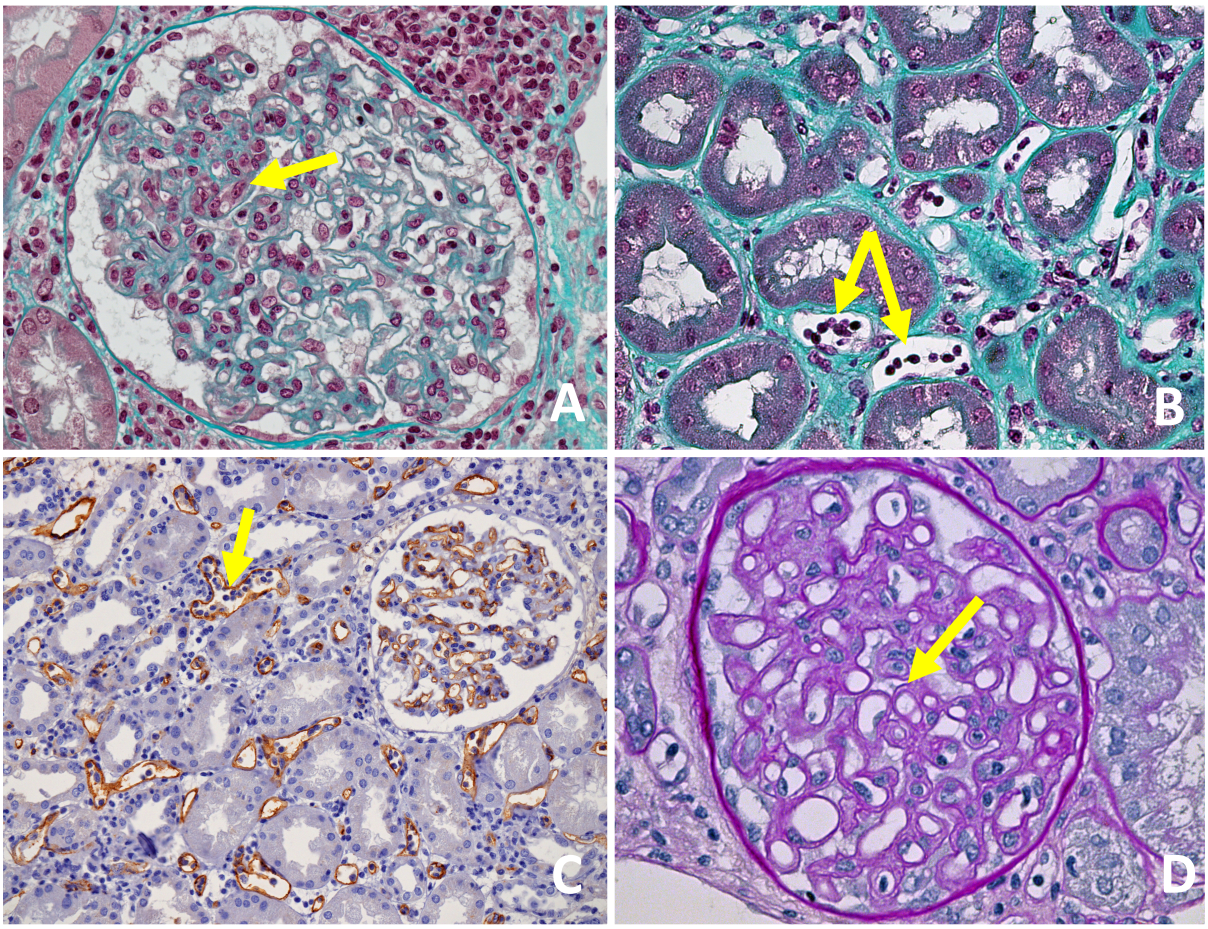

Figure 6* : Lésions élémentaires retrouvées au cours du rejet humoral en transplantation rénale

A : Glomérulite segmentaire, trichrome de Masson, grossissement d'origine x400. Des cellules inflammatoires comblent la lumière d'une partie des anses capillaires (flèche). B : Capillarite péritubulaire, trichrome de Masson, grossissement d'origine x400. De multiples cellules inflammatoires sont retrouvées au sein des capillaires péritubulaires (flèche). C : Immunomarquage C4d, grossissement d'origine x200. Présence d'un marquage linéaire et complet sur l'ensemble des capillaires péritubulaires ainsi que glomérulaires. Des lésions de capillarite péritubulaire sont parfois visibles (flèche). D : Glomérulopathie d'allogreffe, score cg3, coloration à l'acide périodique de Schiff, grossissement d'origine x400. La membrane basale glomérulaire apparait dédoublée (aspect en rail, flèche) sur la majeure partie des anses capillaires.

D) Problématiques diagnostiques actuelles du rejet humoral en transplantation rénale

Malgré une définition régulièrement actualisée, le diagnostic de rejet humoral en transplantation rénale reste complexe car il représente un groupe lésionnel hétérogène et dynamique, variant de formes infra-cliniques (uniquement dépistées sur des biopsies protocolaires) à fulminantes (4), et du fait de limitations intrinsèques aux critères diagnostiques clés, déterminés par consensus d'experts de façon « empirique », sans validation externe possible en l'absence de *gold standard* diagnostique.

Ainsi les critères morphologiques, glomérulite et capillarite péritubulaire, souffrent d'une reproductibilité inter-observateur respectivement faible (k = 0,31) et modérée (k = 0,49), même entre pathologistes spécialisés (19,20). Quant aux dépôts de C4d au niveau des capillaires péritubulaires, bien que très spécifiques du rejet humoral et corrélés à la perte du greffon, ceux-ci restent peu sensibles, étant négatifs dans 20% (19) à 60% des cas suivant les séries (15). C'est d'ailleurs pourquoi la classification de Banff reconnaît le rejet humoral C4d négatif depuis 2013, utilisant l'inflammation modérée de la microcirculation ($g + cpt \geq 2$) comme principal marqueur de substitution.

Le développement des techniques de biologie moléculaire, essentiellement par l'étude du transcriptome, a permis une nouvelle caractérisation physiopathologique du rejet d'allogreffe, et notamment de son versant humoral, *via* l'étude de transcrits de gènes spécifiques (21,22). Au cours du rejet humoral, les transcrits surreprésentés ont été associés pour l'essentiel à l'activation des cellules endothéliales, des macrophages et des cellules NK. Cette approche moléculaire du rejet humoral a d'ailleurs bénéficié d'un transfert clinique et fait maintenant partie intégrante de la classification de Banff (23), comme marqueur de substitution à l'interaction des anticorps du patient avec l'endothélium du greffon et/ou aux DSA (critères 2 et 3, cf. *supra*).

Un exemple de classificateur moléculaire est celui de l'équipe d'Edmonton, qui a ainsi développé un outil diagnostique du rejet humoral sur biopsie congelée, basé sur une technique d'analyse transcriptomique large spectre par *microarrays*, baptisé « Microscope Moléculaire ». Testé de manière prospective, il a montré une meilleure corrélation avec la survie du greffon que les critères diagnostiques conventionnels (21,22). Cette étude, effectuée sur une large série de près de 500 biopsies, a montré une concordance de 77% dans le diagnostic du rejet humoral entre l'approche transcriptomique et les critères conventionnels. Sur les cas discordants, il est estimé par les cliniciens que cette technique aurait pu influencer le traitement pour une proportion considérable de patients (39% des cas), bien qu'il ne soit pas possible d'en prédire l'impact.

Néanmoins cette approche n'est pas exempte de limitations. La nécessité de disposer de matériel biopsique frais ou congelé dédié, et donc de réaliser une troisième biopsie pour un même patient (pour la microscopie optique, pour l'immunofluorescence et pour l'analyse transcriptomique) peut être à l'origine d'une morbidité accrue (0,5-1 % de complications graves post-biopsiques). De plus, à l'heure actuelle, cette technique est difficilement applicable en routine au sein des différents centres d'analyse

spécialisés, car requiert non seulement une plateforme de biologie moléculaire et du matériel biopsique frais ou congelé, mais nécessite également une mise au point et une validation technique indépendante pour chaque centre, en l'absence de standardisation des méthodes d'analyse transcriptomique proposée (7) : quel panel de gènes analyser, nombre de transcrits à analyser, sensibilité technique, seuils de positivité diagnostique, ... Enfin, le coût d'analyses transcriptomiques à large spectre reste élevé. Des signatures moléculaires restreintes sur tissu fixé en formol et inclus en paraffine (FFPE), type NanoString™, se développent (24) afin de pallier ces difficultés. La toute récente naissance du panel de gènes B-HOT (*Banff-Human Organ Transplant*), dédié à l'analyse moléculaire des biopsies en transplantation d'organes solides par la plateforme NanoString™, est actuellement annoncée comme la future référence en pratique clinique (25). La classification de Banff retient ainsi l'approche moléculaire sur tissu FFPE dans le diagnostic des lésions de rejet comme un axe de recherche clef pour les années futures.

E) Intérêts d'une approche protéomique dans la caractérisation du rejet humoral

Les techniques d'analyse protéomique par spectrométrie de masse permettent d'analyser le profil d'expression protéique de tissus (biopsies ou pièces opératoires) mais également de prélèvements non-invasifs (liquides biologiques). Par rapport au transcriptome, l'un des intérêts du protéome est de représenter un compartiment plus fonctionnel (26), en détectant les molécules biologiquement actives, les protéines, et en s'affranchissant des modulations d'expression génique post-transcriptionnelles. Ainsi les modulations des taux d'ARN expliqueraient seulement entre 30 à 40% des modifications d'expression protéique (27). La conversion de biomarqueurs identifiés par analyse protéomique vers des techniques de routine de pathologie (immunohistochimie) peut également se faire de façon plus directe.

L'amélioration récente de l'extraction des protéines à partir de prélèvements tissulaires FFPE (28) a révélé tout l'intérêt de cette approche pour la recherche clinique, considérant l'importante ressource de prélèvements archivés dans les laboratoires d'Anatomie Pathologique. La faisabilité d'une analyse protéomique sur prélèvement FFPE a également l'avantage majeur de permettre un contrôle histologique précis du tissu analysé, à l'inverse d'une analyse sur biopsie congelée, d'interprétation perturbée par les artéfacts de cryopréservation, voire réalisée sans contrôle morphologique du tissu analysé, alors que les lésions de rejet peuvent être focales. Associée à des techniques de microdissection laser sur lames colorées, l'analyse protéomique peut ainsi être ciblée sur les cellules/tissus d'intérêt, limitant la variabilité inter-échantillon et augmentant la robustesse de l'analyse.

Cette combinaison technique a d'ores et déjà démontré son intérêt dans la recherche de biomarqueurs spécifiques d'entités lésionnelles, en pathologie tumorale (29) ou non (30). Ainsi en pathologie rénale inflammatoire, la microdissection laser glomérulaire couplée à la spectrométrie de masse en tandem a permis l'identification de la protéine *DnaJ Homolog Subfamily B Member 9*

(DNAJB9) comme biomarqueur diagnostique de la glomérulonéphrite fibrillaire par deux équipes indépendantes (31,32). Son expression est facilement identifiable par outil immunohistochimique sur biopsie, et permet donc un diagnostic simple de cette glomérulopathie, jusque-là restreint à la microscopie électronique, technique lourde et chronophage. Plus récemment encore, cette technique a également permis l'identification des biomarqueurs Exostosin1/2 comme possibles auto-antigènes d'un sous-groupe de glomérulonéphrite extra-membraneuse (33).

En transplantation rénale, quelques études ont analysé le protéome d'échantillons sanguins et/ou urinaires à la recherche de biomarqueurs avec l'objectif d'un diagnostic non invasif du rejet humoral (26,34), restant sans application clinique actuellement. Les études du protéome tissulaire rénal restent marginales dans le domaine de la transplantation, et ont cherché à caractériser les mécanismes moléculaires du rejet chronique non actif (35), ou encore les lésions restant inéluctables de fibrose interstitielle et d'atrophie tubulaire (36), qui grèvent la fonction du greffon à long terme.

A notre connaissance, cette étude est la première à s'intéresser spécifiquement au protéome glomérulaire au cours du rejet humoral en transplantation rénale à partir de prélèvements biopsiques FFPE.

II- Original Article

A) Title and co-authors

Identification of new immunomarkers of active antibody-mediated rejection through glomerular proteome analysis in kidney transplantation

Authors:

Bertrand Chauveau[1,2], Anne-Aurélie Raymond[3,4], Sylvaine Di Tommaso[3,4], Jonathan Visentin[2,5], Agathe Vermorel[6], Nathalie Dugot-Senant[7], Cyril Dourthe[3,4], Jean-William Dupuy[8], Julie Déchanet-Merville[2], Lionel Couzi[2,6], Frédéric Saltel[3,4], Pierre Merville[2,6]

Affiliations:

[1] Department of Pathology, University Hospital of Bordeaux, Bordeaux, France

[2] CNRS-UMR 5164 ImmunoConcEpT, Bordeaux University, Bordeaux, France

[3] Plateforme Oncoprot, TBM-Core US 005, 33000 Bordeaux, France

[4] INSERM, UMR1053, BaRITOn Bordeaux Research in Translational Oncology, Bordeaux, France

[5] Department of Immunology and Immunogenetics, Bordeaux University Hospital, Bordeaux, France

[6] Department of Nephrology, Transplantation, Dialysis and Apheresis, University Hospital of Bordeaux, Bordeaux, France

[7] Plateforme d'histologie UMS 005, Bordeaux, France

[8] Plateforme Protéome, Bordeaux University, Bordeaux, France

B) Introduction

In the overwhelming context of organ shortage, improving long-term allograft survival is a major issue in kidney transplantation (37). Over the past decade, antibody-mediated rejection (ABMR) has been pointed out as the leading cause of kidney allograft failure, thought to be involved in about two-thirds of cases (2).

ABMR is primary an endothelial disease, where donor-specific antibodies (DSA), targeting human leukocyte antigens (HLA) or other antigens, bind to endothelial cell surface, leading to the recruitment of inflammatory cells and injuries (from activation to cell lysis), whether or not complement-mediated (4,15). According to the 2019 Banff classification, the diagnosis of active ABMR relies on both histological and biological criteria (18). Validated molecular classifiers have been added since 2015 (38), although they are not for now widely available. Thus, for many centers the hallmarks

remain on the one hand the histological lesions, with at least a moderate microvascular inflammation (MVI), namely glomerulitis and/or peritubular capillaritis, and C4d deposits on peritubular capillaries, and on the other hand the detection of DSA in the serum of the patient. The diagnosis can be retained when not all criteria are present, as proposed surrogate markers allow several combinations to be accepted as diagnostic. However the diagnosis of active ABMR remains complex, because of our limited understanding of the full dynamic range of ABMR and the known limitations of the current hallmark criteria. Indeed, the morphological scores of glomerulitis and peritubular capillaritis still lack inter-observer reproducibility, even between advanced nephropathologists (19,20). C4d deposits on peritubular capillaries display high specificity for an active antibody-mediated mechanism, but their lack of sensitivity is well known (15,19). Considering the DSA criterion, the heterogeneity between centers in the exhaustivity of their testing and the growing evidences of the involvement of non anti-HLA antibodies in ABMR (10), which are not easily routinely tested, prompted to recognize active ABMR with no DSA detectable since the 2017 Banff classification (38).

There is so an unmet need for alternative approaches to improve in daily practice the diagnostic accuracy of active ABMR (aABMR) in kidney transplantation. During the last years transcriptomic analyses from frozen samples proved their usefulness in this setting (39,40). They highlighted the major involvement of macrophages and NK cells, interferon gamma and activated endothelial cells during aABMR, revealed its C4d negative phenotype (15), and even managed a real time assessment of kidney allograft biopsy as a proof of concept (22). Still their worldwide availability remains for now an issue. Otherwise, development of mass spectrometry-based proteomics allows an exhaustive description of protein expression abundance, as such taking into account post-transcriptional and translational gene expression modifications (27), that can directly be linked to phenotypes of complex injuries. Proteomics analyses can be performed from formalin-fixed and paraffin embedded (FFPE) samples (28), allowing a quality morphological control from the same analyzed sample. Combining mass spectrometry with a previous laser microdissection of the samples allows the identification of the proteome of a very specific tissue or cell compartment, thus reducing inter-samples variability for a more robust analysis (29,41). In the field of kidney diseases, such approaches have been recently successful in the identification of DNAJB9 as an immunohistochemical diagnostic marker of fibrillary glomerulonephritis (31,42), and of a new couple of immunomarkers, Exostosin 1/Exostosin 2, in a subset of membranous nephropathy (33).

As glomerulitis is the most specific morphological lesion in aABMR, we performed the "GlomProt" pilot study, using laser microdissection coupled with tandem mass spectrometry-based proteomics from FFPE biopsies, to describe the protein profile of anti-HLA antibody-mediated glomerular injuries in human kidney transplantation and to identify potential immunomarkers of ABMR diagnosis for daily practice.

C) Methods

a- Selection of the cohorts

Two independent cohort were selected, one for the mass spectrometry analysis and the identification of immunomarkers and the other for the assessment of immunomarkers performances in the diagnosis of aABMR by immunohistochemistry. All included cases consisted of renal allograft biopsies, already performed for diagnosis purposes from March 2010 to April 2019 at the Bordeaux University Hospital.

The cohort for the mass spectrometry analysis and the identification of immunomarkers consisted of two groups: aABMR (n=24) and stable graft (SG) controls (n=10). For each group, cases were selected based on the number of permeable glomeruli in the sample, with a minimum of 10 *per* section. The diagnoses of aABMR were in accordance with the 2015 Banff classification, but also all selected biopsies were with a glomerulitis score greater than or equal to 1 ($g \geq 1$), and all patients of this group had at least one anti-HLA DSA in their serum at the time of the diagnosis of rejection. Biopsies with mixed rejection, displaying thus both aABMR and acute T-cell mediated rejection were not included, but borderline infiltrate was admitted. Biopsies included in the SG group consisted of one year protocol biopsies in patients with an eGFR greater than 40 mL/min/1.73 m^2, no clinical proteinuria (lesser than 50 mg/mmol), no anti-HLA DSA in their serum and without history of rejection or BK virus infection. These samples had no microvascular inflammation, no acute tubulo-interstitial inflammation, no chronic glomerular lesion (cg0, mm0). Moderate interstitial fibrosis and tubular atrophy (IFTA) and moderate chronic vascular lesions were tolerated. For all cases immunofluorescence study with antibodies targeting IgA, IgG, IgM, C3, Kappa and Lambda was negative. C4d status was assessed by immunoperoxidase. We also processed a “normal” native renal surgical specimen, obtained from a patient who underwent a total nephrectomy for a renal cell carcinoma, without morphological glomerular injuries. The sample was collected several centimeters from the tumor site. It was thought as a calibrator in case of technical issue (chromatographic drift) during spectrometric data acquisition.

The independent cohort for the assessment of immunomarkers performances using immunohistochemistry was selected in accordance with the 2015 Banff classification, regardless of the glomerulitis score, with at least 8 glomeruli based on the histopathology report, and was composed of 53 cases with 16 active ABMR cases (including 5 C4d positive) and 37 relevant differential diagnoses: T-cell mediated rejections (n=6), infections (3 polyomavirus nephropathies and 2 acute pyelonephritides), acute tubular injuries (n=5), recurrent or *de novo* glomerulopathies (3 IgA nephropathies and 2 membranous nephropathies), non-humoral thrombotic microangiopathies (n=5), isolated C4d positivity (n=3), chronic ABMR without activity (especially g0 cpt0, n=5) and stable graft cases in ABO incompatible transplantation (one year protocol biopsies without acute lesion, n=3). According to the local institutional ethics board requirement, patients for whom kidney biopsy was

eligible were contacted and had the legal time to express their opposition. Clinical data were collected thanks to the local medical software for which all patients signed a written informed consent.

b- Laser microdissection

Biopsy samples were already fixed in 4% acetic formalin and paraffin-embedded, as tissue sections were routinely processed for diagnosis purposes. For each sample, 5 µm thick sections were performed and deposited on PEN Membrane Glass Slides (Thermo Fisher Scientific, California, USA). The sections were then dewaxed, rehydrated and stained with hematoxylin. For each replicate, 50 non globally sclerotic glomerular sections were isolated using the PALM MicroBeam (Zeiss) laser microdissector. Two replicates were performed for each biopsy, and a total of nine replicates were performed for the normal kidney (surgical specimen).

c- Protein extraction and sample preparation for mass spectrometry

The steps of sample preparation and protein digestion were performed as previously described (29). Microdissected tissues were incubated in a Tris-HCl pH 6,8 solution for 2 hours at 95°C, including a sonication stage. Samples were loaded on a 10% acrylamide SDS-PAGE gel. Migration was stopped when the samples entered the resolving gel and the proteins were visualized by colloidal blue staining. Each band of gel was then digitized, and the optical density was measured to allow a standardization of the protein amount before mass spectrometry. Each SDS-PAGE band was cut into 1 mm x 1 mm gel pieces. Gel pieces were destained in 25 mM ammonium bicarbonate (NH4HCO3), 50% acetonitrile (ACN) and shrunk in ACN for 10 minutes. After ACN removal, the gel pieces were dried at room temperature. The proteins were first reduced in 10 mM dithiothreitol, 100 mM NH4HCO3 for 30 minutes at 56°C then alkylated in 100 mM iodoacetamide, 100 mM NH4HCO3 for 30 minutes at room temperature and shrunk in ACN for 10 minutes. After ACN removal, the gel pieces were rehydrated with 100 mM NH4HCO3 for 10 minutes at room temperature. Before protein digestion, the gel pieces were shrunk in ACN for 10 minutes and dried at room temperature. The proteins were digested by incubating each gel slice with 10 ng/µL of trypsin (T6567, Sigma-Aldrich) in 40 mM NH4HCO3, 10% ACN, rehydrated at 4°C for 10 minutes, and were finally incubated overnight at 37°C. The resulting peptides were extracted from the gel in three steps: the first incubation was in 40 mM NH4HCO3, 10% ACN for 15 minutes at room temperature and two subsequent incubations were in 47.5 % ACN, 5% formic acid for 15 minutes at room temperature. The three collected extractions were pooled with the initial digestion supernatant, dried in a SpeedVac, and re-suspended in 0.1% formic acid before nanoLC-MS/MS analysis. The volume of re-suspension varied from 15 to 43 µL, depending of the measured optical density of the initial electrophoresis gel.

d- Proteomic analysis

Mass Spectrometry-based proteomic analysis of the samples was performed as described previously (29). NanoLC-MS/MS analysis was performed using an Ultimate 3000 RSLC Nano-UPHLC system (Thermo Scientific, USA) coupled to a nanospray Orbitrap Fusion™ Lumos™ Tribrid™ Mass Spectrometer (Thermo Fisher Scientific, California, USA). Each peptide extracts were loaded on a 300 µm ID x 5 mm PepMap C18 precolumn (Thermo Scientific, USA) at a flow rate of 10 µL/min. After a 3 min desalting step, peptides were separated on a 50 cm EasySpray column (75 µm ID, 2 µm C_{18} beads, 100 Å pore size, ES803, Thermo Fischer Scientific) with a 4-40% linear gradient of solvent B (0.1% formic acid in 80% ACN) in 55 min. The separation flow rate was set at 300 nL/min. The mass spectrometer operated in positive ion mode at a 2.0 kV needle voltage. Data was acquired using Xcalibur 4.1 software in a data-dependent mode. MS scans (m/z 375-1500) were recorded at a resolution of R=120000 (@ m/z 200) and an AGC target of $4x10^5$ ions collected within 50 ms, followed by a top speed duty cycle of up to 3 seconds for MS/MS acquisition. Precursor ions (2 to 7 charge states) were isolated in the quadrupole with a mass window of 1.6 Th and fragmented with HCD@30% normalized collision energy. MS/MS data was acquired in the Orbitrap cell with a resolution of R=30000 (@m/z 200), AGC target of $5x10^4$ ions and a maximum injection time of 100 ms. Selected precursors were excluded for 60 seconds. For protein identification, we have used Mascot 2.5 algorithm available through Proteome Discoverer 1.4 Software (Thermo Fisher Scientific Inc.). It was used in batch mode by searching against the UniProt Homo sapiens database (73 658 entries, Reference Proteome Set, release date: December 13, 2018) from http://www.uniprot.org/ website. Two missed enzyme cleavages were allowed. Mass tolerances in MS and MS/MS were set to 10 ppm and 0.02 Da. Oxidation of methionine, acetylation of lysine and deamidation of asparagine and glutamine were searched as dynamic modifications. Carbamidomethylation on cysteine was searched as static modification. Raw LC-MS/MS data were imported in Proline Studio (43) for feature detection, alignment, and quantification. Proteins identification was accepted only with at least 2 specific peptides with a pretty rank=1 and with a protein FDR value less than 1.0% calculated using the “decoy” option in Mascot. Label-free quantification of MS1 level by extracted ion chromatograms (XIC) was carried out with parameters indicated previously (29). The normalization was carried out on median of ratios. The inference of missing values was applied with 5% of the background noise.

e- Immunohistochemical analysis

Biopsy samples were already fixed in 4% acetic formalin as tissue sections were routinely processed for the purpose of diagnosis. For immunohistochemistry, 2.5 µm thick sections were performed, dewaxed and rehydrated. Antigen retrieval was performed in a 1mM Tris-EDTA pH9 solution. All staining procedures were performed in an automated autostainer (Dako-Agilent Clara, United States) using standard reagents provided by the manufacturer. Five commercial antibodies were

used against: Tryptophanyl tRNA synthetase/WARS (clone EPR3423, Abcam, dilution 1:3000), Coronin1a/TACO (clone EPR19467-36, Abcam, 1:3000), Thymidine Phosphorylase/TYMP (clone P-GF.44C, Abcam, 1:200), EF-hand domain family member 2/EFHD2 (rabbit polyclonal, Sigma-Aldrich, dilution 1:200) and Guanylate-binding protein 1/GBP1 (clone OTI1B2, Abcam, dilution 1:50). The sections were incubated with the corresponding antibody for 45 min at room temperature. EnVision Flex/HRP (Horseradish peroxidase) (Dako-Agilent, 20 minutes) was used for signal amplification. 3,3'-Diamino-benzidine (DAB, Dako) development was used for detecting primary antibodies. The slides were counterstained with hematoxylin, dehydrated and mounted. Each immunohistochemical run contained a negative (buffer, no primary antibody) and positive control. Immunostainings images were acquired using the NIS-Elements D 3.10 software, with a Nikon Eclipse 80i microscope.

Histological glomerular scores evaluating the global intensity of staining were assessed. For the WARS, GBP1 and TYMP antibodies, the histological scores were calculated for each case by assessing the mean intensity of staining of the glomeruli, by visually evaluating the number of positive glomeruli and their respective intensity of staining (0 to 3+) compared to the total number of glomeruli in the biopsy. Only cases with a minimum of 4 permeable glomeruli were considered for this semi-quantitative evaluation. For the CORO1A and EFHD2 antibodies, the histological score was assessed by calculating the mean number of positive cells per glomerulus with a visual enumeration. Only cases with at least 8 permeable glomeruli were assessed for this quantitative enumeration of such often focal lesions like glomerulitis.

As for evaluating the performances of the antibodies in the diagnosis of active ABMR, the immunomarkers slides from the independent cohort were interpreted by two nephropathologists, (BC and AV). They were unaware of the diagnosis and should assess each case as positive or negative for an active ABMR process. For each antibody, the training set consisted of the immunostainings obtained from the spectrometric-analyzed cohort.

f- Bioinformatical analysis of proteomics data

Non-parametric Mann-Whitney U tests were used to compare the protein abundance distribution between the two groups. For each duplicate, only the mean protein abundance was considered. P-values were further corrected using the Benjamini-Hochberg multiple test correction algorithm (44), and the threshold of statistical significance was considered at 0.05. To study the protein association networks, we used the online resource STRING (version 11.0) (45), using the default settings, retaining the biological processes as defined by the Gene Ontology terminology from their corresponding False Discovery Rate (FDR), with a threshold of significance considered at 0.05. As such a significant biological process means that the corresponding proteins have more interactions among themselves than what would be expected for a random set of proteins of similar size, indicating that they are at least partially biologically connected. We also performed a pathway analysis using the Ingenuity Pathway

Analysis software (IPA, Qiagen). Proteins interactions were then exported from STRING and adapted with the Cytoscape software, version 3.7.1, using default settings, to integrate all pathway analyses.

A supervised classification method by Random Forests, using the R package "randomForest", version 4.6-14 (46), was performed to select relevant proteins of aABMR. Classification Random Forest algorithms build many decision trees to establish a robust classifier. For each tree, a subset of samples is selected to build the tree ("in-bag" samples); each node is split using the best among a predetermined number of variables randomly chosen at that node. The remaining samples ("out-of-bag") are predicted from this tree, allowing an estimation of the error rate. For each tree, a bootstrap iteration defines the "in-bag" samples from the "out-of-bag" ones. Aggregating the "out-of-bag" (OOB) predictions defines the OOB estimate of error rate. The final classification of each case of the training dataset by the established model is easily readable in a confusion matrix, with a simple majority vote taken for prediction. Herein the algorithms were set to distinguish the ABMR samples from the SG ones (classification type). Several algorithms were defined to progressively select the most discriminant variables while checking the classification performances.

All statistical analyses were performed using the R software, version 3.6.0 (47). Correlations were assessed using the cor.test function.

D) Results

a- Demographical characteristics of the active ABMR and stable graft groups

We initially included 34 patients whose allografts had been biopsied from April 2011 to September 2018. We secondarily excluded 5 patients: 3 due to a lack of remaining material in the paraffin block, one due to a positive BK viremia at the time of biopsy and one because of inexploitable spectrometric data. On the 29 remaining patients, 4 (14%) had only one exploitable replicate after spectrometric acquisition. The fully detailed flow-chart of the study is described in Supplemental Figure S1. Overall there were 21 patients in the aABMR group and 8 in the SG group. The relevant clinical, biological and histological characteristics are summarized in Table 1. Of note, 7 cases (33%) in the aABMR group were C4d positive and 14 patients (67%) had *de novo* DSA at the time of biopsy. Ten biopsies in this lesional group (48%) also showed evidence of chronic active antibody-mediated lesions (at least cg1b).

b- Proteomics analysis of active antibody-mediated glomerular injuries

Overall 1335 proteins were identified from the different analyzed samples and quantified for all samples (no missing data). From this global glomerular proteome, 232 proteins were differentially represented in the aABMR group compared to the SG one (adjusted p-value < 0.05). We retained 82

proteins, characterized by 54 (66%) significantly overrepresented proteins (fold change above 2) and 28 (34%) underrepresented (fold change below 0.5) in the aABMR group. In accordance with adjusted p-values, the top-25 most significant proteins are presented in Table 2 and the 82 protein set in Supplemental Table S1. The study of the protein association networks using the STRING online resource identified the major involvement of the immune response, with 23 directly immune-related proteins from the 82 set (28%, immune system process, FDR=0.0052) and especially 18 from the 54 overrepresented proteins (33%, immune system process, FDR=0.005). In this latter group, the enrichment process particularly highlighted relevant immune-related biological processes such as defense response to virus (FDR=8.35E-05), type I interferon pathway (FDR=0.0008), regulation of T-cell proliferation (FDR=0.0296), regulation of leukocyte cell-cell adhesion (FDR=0.0338) and response to interferon-gamma (FDR=0.0375). Other relevant biological processes from the overrepresented proteins included regulation of cytoskeleton organization (FDR=0.0012), translation (FDR=0.0225) and blood vessel morphogenesis (FDR=0.0258). Regarding the underrepresented proteins, they mainly referred to small molecule metabolic process (FDR=3.47E-05) such as cellular amino acid metabolic (FDR=3.29E-07), catabolic (FDR=5.13E-05) and oxidation-reduction processes (FDR=0.0013). We then used the Ingenuity Pathway Analysis software, which mainly identified EIF2 signaling (p=1.74E-03), the role of PKR in interferon induction and antiviral response (p=2.45E-03) and interferon signaling (p=3.09E-03) in overrepresented proteins and notably LPS/IL-1 mediated inhibition of RXR function (p=7,24E-06) and glutathione-mediated detoxification (p=7.08E-04) in underrepresented proteins. Most relevant STRING results for the overrepresented proteins are presented in Table 3 (all results are shown in Supplemental Table S2 for overrepresented and Supplemental Table S3 for underrepresented proteins). An overall and integrative visual summary of the most significant pathways involved in antibody-mediated glomerular lesions is presented in Figure 1.

c- Identification of surrogate immunomarkers of active ABMR

To select the most relevant immunomarkers of active ABMR from the proteomics dataset, we combined two selection methods: first the most statistically significant proteins retained from the aABMR/SG comparison (as already shown in Table 2) and second the most important proteins according to a supervised classification random Forest model. For this latter, we established a random Forest model, combining the 10 most discriminating proteins from the whole dataset, which was able to classify all samples in their corresponding group (aABMR and SG), for an out-of-bag estimate of error rate of 0%. The relative importance of each protein from this model is showed in Supplemental Figure S2. Both methods focused on 5 proteins that were selected for immunohistochemistry testing: thymidine phosphorylase (TYMP), tryptophan--tRNA ligase, cytoplasmic (WARS), coronin-1A (CORO1A), guanylate-binding protein 1 (GBP1) and EF-hand domain-containing protein D2 (EFHD2). Tubulointerstitial nephritis antigen (TINAG) was not selected because an underrepresentation (fold

change aABMR/SG=0.35) is often considered more difficult to interpret than the reverse by immunohistochemistry. Despite the relative importance of prostatic acid phosphatase (ACPP) according to the random Forest model, the fold change aABMR/SG of 1.43 was considered insufficient for an immunohistochemistry practice, and prompted us to unselect it. The Figure 2 shows the relative protein abundance for all samples, as acquired by the mass spectrometer, depending on the group, for the 5 selected proteins, exhibiting an obvious overrepresentation of these proteins in the aABMR group.

d- Kidney graft expression of WARS, TYMP, GBP1, CORO1A and EFHD2 in active antibody-mediated rejection

To demonstrate the overrepresentation proposed by the mass spectrometer, we performed an immunohistochemistry study of the five selected proteins within the mass spectrometric cohort, in all samples with sufficient remaining material. As shown in the example of Figure 3, all five antibodies showed a cytoplasmic positivity and to some extent nuclear. They all stained inflammatory infiltrates, but with various strength and pattern (diffuse, focal or scattered cells), whether in the glomeruli or not. CORO1A and EFHD2 almost exclusively stained inflammatory cells, almost all for CORO1A, much less for EFHD2 (scattered pattern). A histological glomerular score was assessed for each slide and each antibody by a pathologist (BC) to quantify their *in situ* expression. Details about the histological scores are provided in the Methods section. A significant correlation between the histological glomerular score and the spectrometric protein abundances was noted for all antibodies, with a Spearman's correlation coefficient, ρ=0.80 (p=1.6E-05) for the WARS antibody (n=21 analyzed cases), ρ=0.90 (p=3.7E-06) for the TYMP antibody (n=22) and ρ=0.93 (p=1.9E-08) for the GBP1 antibody (n=18). Pearson's correlation coefficient, r, was of 0.85 (p=4.9E-05) for the CORO1A antibody (n=15) and r=0.83 (p=1.5E-04) for the EFHD2 antibody (n=15). The detailed expression pattern of these five antibodies, as seen in this spectrometric cohort, is proposed in Table 4. Interestingly WARS, TYMP and GBP1 also stained endothelial cells in the aABMR cases, both in glomeruli and peritubular capillaries, even without prominent inflammatory cells, leading us to further consider them for diagnostic purposes, as their enhanced expression could represent endothelial stress.

e- Diagnostic performances of WARS, TYMP and GBP1 in the diagnosis of active ABMR in kidney transplantation by immunohistochemistry

We used an independent retrospective cohort to evaluate WARS, TYMP and GBP1 in the diagnosis of aABMR by immunohistochemistry. This cohort was composed of 53 cases, 16 aABMR (including 5 C4d positive) and 37 various differential diagnoses, as depicted in the Methods section. Two pathologists (BC and AV), unaware of the diagnosis, interpreted the slides as positive or negative for aABMR diagnosis. As these antibodies are novel in the field of graft pathology and each has his own pattern of expression, the slides set from the spectrometric cohort served as a training cohort for the

pathologists, in order to adopt common criteria for positivity. TYMP and WARS positivity required a strong and diffuse endothelial staining in at least one microcirculation compartment (either glomeruli and/or peritubular capillaries). GBP1 positivity was considered when either at least a third of a microcirculation compartment was strongly stained, even if segmental, or showed a diffuse weak staining. For all antibodies, peritubular capillaries staining should not be assessed in area of marked tubulo-interstitial inflammation, where non-specific endothelial positivity was observed. The results are summarized in Table 5. Fully detailed results are exposed in Supplemental Tables S4/S5, S6/S7 and S8/S9 respectively for WARS, TYMP and GBP1, with the detailed interpretation results and the final diagnostic performances. TYMP had overall the best diagnostic performances, with a mean sensitivity (Se) of 82% and specificity (Sp) of 88%, with a strong agreement (Cohen's κ=0.7). WARS was slightly less sensitive but still specific (mean Se=72%, Sp=85%) with a fair agreement (κ=0.567). GBP1 was the less sensitive despite good specificity (mean Se=64%, Sp=88%) and the less reproducible (κ=0.511). Misclassifications were mainly due to either marked interstitial inflammation which led to an endothelial positivity on peritubular capillaries, or chronic antibody-mediated rejection cases thought to be non-active according to the Banff classification (Supplemental Figures S3, S4 and S5).

Table 1. Demographical characteristics of aABMR and stable graft patients

	aABMR group (n=21)		Stable graft group (n=8)	
	n		***n***	
Recipient				
Age at the time of biopsy, year, median [IQR]	21	61 [51-70]	8	50 [36-67]
Male, *n* (%)	21	15 (71)	8	5 (63)
ESRD causes, *n* (%)	21		8	
Glomerulonephritis		6 (29)		1 (13)
Diabetes		0 (0)		0 (0)
Polycystic kidney disease		6 (29)		3 (38)
Tubulo-interstitial disease		4 (19)		2 (25)
Vascular nephropathy		2 (10)		0 (0)
Unknown		3 (27)		1 (13)
Other		0 (0)		1 (13)
Prior transplantation, *n* (%)	21	7 (33)	8	2 (25)
Donor				
Age, year, median [IQR]	16	58 [50-64]	6	44 [34-60]
Men, *n* (%)	15	7 (47)	7	3 (43)
Living donor, *n* (%)	19	3 (16)	7	3 (43)
HLA antibody at the time of transplantation	13		8	
No evidence of anti-HLA antibodies, *n* (%)		4 (31)		6 (75)
Evidence of anti-HLA antibodies but not DSA, *n* (%)		2 (15)		2 (25)
DSA, *n* (%)		7 (54)		0 (0)
DSA at the time of the ABMR diagnosis	21		8	
DSA, *n* (%)		21 (100)		0 (0)
DSA class I, *n* (%)		5 (24)		0 (0)
DSA class II, *n* (%)		18 (86)		0 (0)
De novo DSA, *n* (%)		14 (67)		0 (0)
DSA MFI, median [IQR]	21	3047 [984-11477]	8	0 [0-0]
Clinical and biological parameters at the time of biopsy				
Months post-transplantation of biopsy, median [IQR]	21	43.7 [9-84]	8	12 [12-13]
Biopsy indication	21		8	
For cause, *n* (%)		14 (67)		0 (0)
Protocol, *n* (%)		7 (33)		8 (100)
eGFR at diagnosis, ml/min/1.73 m^2, median [IQR]	21	35 [22-46]	8	76.5 [52-82]
Proteinuria at diagnosis, mg/mmol, median [IQR]	19	89 [37-234]	8	10 [8-14]
Immunosuppression at the time of biopsy, *n* (%)	21		8	
Tacrolimus		14 (67)		6 (75)
Cyclosporin A		6 (29)		2 (25)
Everolimus		4 (19)		1 (13)
Azathioprin		1 (5)		1 (13)
MMF		16 (76)		6 (75)
Corticosteroids		16 (76)		5 (63)
Tacrolimus and MMF		13 (62)		4 (50)
Histological parameters				
Total number of glomeruli, median [IQR]	21	18 [13-21]	8	16 [15-18]
Number of globally sclerotic glomeruli, median [IQR]	21	1 [0-1]	8	0 [0-0.3]
Banff scoring				
g, mean (SD)	21	1.7 (0.6)	8	0 (0)
cpt, mean (SD)	21	1.8 (0.8)	8	0 (0)
cg, mean (SD)	21	1.1 (1.3)	8	0 (0)
mm, mean (SD)	21	0.8 (0.9)	8	0 (0)

Table 1. Demographical characteristics of aABMR and stable graft patients (continued)

	aABMR group (n=21)		Stable graft group (n=8)	
	n		***n***	
C4d positivity on the peritubular capillaries, *n* (%)	21	7 (33.3)	7	0 (0)
i, mean (SD)	21	0.4 (0.7)	8	0 (0)
t, mean (SD)	21	0.3 (0.8)	8	0 (0)
v, mean (SD)	20	0.1 (0.4)	6	0 (0)
ci, mean (SD)	21	1.3 (0.7)	8	0.6 (0.7)
ct, mean (SD)	21	1.3 (0.7)	8	0.6 (0.7)
ah, mean (SD)	21	1 (1.3)	8	0.8 (0.9)
cv, mean (SD)	20	1.3 (1.1)	6	1.2 (1)
C4d positivity on the glomeruli, mean (SD)	21	1.3 (1.2)	7	0.3 (0.5)
Follow-up and clinical evolution				
Follow-up after biopsy, months, median [IQR]	21	28 [14-35]	8	27 [10-36]
eGFR evolution from 6 months before and 6 months after biopsy, median [IQR]	17	-15 [-18- -10]	7	2 [-9-4]
eGFR evolution at the last follow-up, median [IQR]	21	-14 [-19-1]	8	-4 [-12-0]
Allograft failure at 1 year, *n* (%)	20	5 (25)	8	0 (0)
Allograft failure at the last follow-up, *n* (%)	21	8 (38)	8	0 (0)
Death whatever the cause at the last follow-up, *n* (%)	21	1 (5)	8	0 (0)

Abbreviations: ABMR, antibody-mediated rejection; IQR, interquartile range; ESRD, end-stage renal disease; HLA, human leukocyte antigens; DSA, donor-specific antibodies; eGFR, estimated glomerular filtration rate; MFI, mean fluorescence intensity; MMF, mycophenolate mofetil.

Table 2. Top-25 of the 82 protein profile of glomerular injuries in the aABMR group compared to the SG one, in ascending order of adjusted p-values

UniProt access	Full protein name	Corresponding gene name	Ratio of median aABMR/SG	Adjusted p-values
P19971	Thymidine phosphorylase	TYMP	4.15	1.78E-04
Q96C19	EF-hand domain-containing protein D2	EFHD2	5.00	1.78E-04
P23381	Tryptophan--tRNA ligase, cytoplasmic	WARS	2.53	1.78E-04
Q9UJW2	Tubulointerstitial nephritis antigen	TINAG	0.35	1.78E-04
P32455	Guanylate-binding protein 1	GBP1	3.48	2.49E-04
P31146	Coronin-1A	CORO1A	3.56	3.96E-04
Q9ULZ3	Apoptosis-associated speck-like protein containing a CARD	PYCARD	18.78	4.98E-04
P13796	Plastin-2	LCP1	3.90	4.98E-04
A0A087X1J7	Glutathione peroxidase	GPX3	0.43	9.82E-04
P50440	Glycine amidinotransferase, mitochondrial	GATM	0.31	2.21E-03
Q13596	Sorting nexin-1	SNX1	2.04	2.82E-03
P09210	Glutathione S-transferase A2	GSTA2	0.31	2.82E-03
E9PF17	Versican core protein	VCAN	13.57	3.16E-03
P28838	Cytosol aminopeptidase	LAP3	2.01	3.16E-03
P42224	Signal transducer and activator of transcription 1-alpha/beta	STAT1	3.04	3.16E-03
Q9Y3Z3	Deoxynucleoside triphosphate triphosphohydrolase SAMHD1	SAMHD1	2.26	3.16E-03
P52907	F-actin-capping protein subunit alpha-1	CAPZA1	2.11	3.16E-03
P04040	Catalase	CAT	0.48	3.16E-03
H3BM42	Golgi apparatus protein 1, isoform CRA_c	GLG1	9.44	3.91E-03
P43121	Cell surface glycoprotein MUC18	MCAM	2.26	3.91E-03
P17927	Complement receptor type 1	CR1	0.39	3.91E-03
H7C0J5	Centrosomal protein of 104 kDa	CEP104	0.46	3.91E-03
G5E9W9	GTPase IMAP family member 4	GIMAP4	2.24	4.80E-03
A0A0A0MS41	Sideroflexin	SFXN3	7.27	4.80E-03
J3QT28	Mitotic checkpoint protein BUB3 (Fragment)	BUB3	6.40	6.00E-03

Non-parametric Mann-Whitney tests were performed to compare the protein expressions between the active antibody-mediated rejection (aABMR) and stable graft (SG) group. P-values were secondarily adjusted according to the Benjamini-Hochberg correction. A fold change aABMR/SG above 2 implies a significant overrepresentation of the protein in the lesional group, whereas a ratio below 0.5 an underrepresentation. The UniProt access refers to the entry in the UniProt Knowledgebase (UniProtKB, https://www.uniprot.org). Abbreviations: aABMR, active antibody-mediated rejection; SG, stable graft control.

Table 3. Most relevant biological processes (GO terminology) from the 54 significantly overrepresented proteins of antibody-mediated glomerular injuries compared to stable graft controls, adapted from the online resource STRING v11.0, in ascending order of false discovery rate

GO-term	Term description	Observed protein count	Background protein count	False discovery rate	Involved proteins (labels)
GO:0051607	defense response to virus	8	181	8.35e-05	BST2,GBP1,ISG15,OAS3,PTPRC,PYCARD,SAMHD1,STAT1
GO:0002252	immune effector process	13	927	0.00080	BST2,C1QB,CORO1A,GBP1,ISG15,LCP1,LRP1,OAS3,PTPRC,PYCARD,SAMHD1,STAT1,WASF2
GO:0032956	regulation of actin cytoskeleton organization	8	297	0.00080	BST2,CAPG,CAPZA1,CD2AP,CORO1A,LRP1,PYCARD,WASF2
GO:0048519	negative regulation of biological process	30	4953	0.00080	BST2,BUB3,CAPG,CAPZA1,CBX3,CD2AP,CDYL,CORO1A,EFEMP1,EIF2S1,GBP1,GLG1,IDO1,ISG15,LRP1,NSFL1C,NT5E,OAS3,PCNA,PROS1,PSMC1,PTPRC,PYCARD,QARS,RPL36A,RPS28,STAT1,TNC,WARS,WASF2
GO:0060337	type I interferon signaling pathway	5	65	0.00080	BST2,ISG15,OAS3,SAMHD1,STAT1
GO:0051493	regulation of cytoskeleton organization	9	477	0.0012	BST2,CAPG,CAPZA1,CD2AP,CORO1A,LRP1,NSFL1C,PYCARD,WASF2
GO:0045087	innate immune response	10	676	0.0025	BST2,C1QB,CAPZA1,CORO1A,GBP1,ISG15,OAS3,PYCARD,SAMHD1,STAT1
GO:0006952	defense response	13	1234	0.0036	BST2,C1QB,CAPZA1,CORO1A,GBP1,IDO1,ISG15,LRP1,OAS3,PTPRC,PYCARD,SAMHD1,STAT1
GO:0050776	regulation of immune response	11	873	0.0036	BST2,C1QB,FAM49B,GBP1,IDO1,PROS1,PTPRC,PYCARD,SAMHD1,STAT1,WASF2
GO:0001818	negative regulation of cytokine production	6	245	0.0073	BST2,CD2AP,GBP1,IDO1,ISG15,PYCARD
GO:0019221	cytokine-mediated signaling pathway	9	655	0.0076	BST2,CAPZA1,GBP1,ISG15,LCP1,OAS3,PYCARD,SAMHD1,STAT1
GO:0048525	negative regulation of viral process	4	93	0.0122	BST2,ISG15,OAS3,STAT1
GO:0043254	regulation of protein complex assembly	7	425	0.0132	CAPG,CAPZA1,CORO1A,LCP1,PSMC1,PYCARD,WARS
GO:0072673	lamellipodium morphogenesis	2	6	0.0151	SNX1,WASF2
GO:0071345	cellular response to cytokine stimulus	10	953	0.0182	BST2,CAPZA1,CORO1A,GBP1,ISG15,LCP1,OAS3,PYCARD,SAMHD1,STAT1
GO:0006950	response to stress	20	3267	0.0183	BST2,C1QB,CAPZA1,CORO1A,EIF2S1,GBP1,IDO1,ISG15,LRP1,MCAM,OAS3,PCNA,PROS1,PSMC1,PTPRC,PYCARD,SAMHD1,STAT1,TNC,VWA1
GO:0033043	regulation of organelle organization	11	1155	0.0183	BST2,BUB3,CAPG,CAPZA1,CD2AP,CORO1A,LCP1,LRP1,NSFL1C,PYCARD,WASF2
GO:0006412	translation	6	362	0.0225	EIF2S1,EIF3CL,QARS,RPL36A,RPS28,WARS
GO:0006413	translational initiation	4	142	0.0258	EIF2S1,EIF3CL,RPL36A,RPS28
GO:0048514	blood vessel morphogenesis	6	381	0.0258	COL15A1,LRP1,MCAM,TYMP,WARS,WASF2
GO:0042129	regulation of T cell proliferation	4	151	0.0296	CORO1A,IDO1,PTPRC,PYCARD
GO:0060333	interferon-gamma-mediated signaling pathway	3	69	0.0331	GBP1,OAS3,STAT1
GO:1903037	regulation of leukocyte cell-cell adhesion	5	278	0.0338	CORO1A,FAM49B,IDO1,PTPRC,PYCARD
GO:0016477	cell migration	8	812	0.0376	CD2AP,CORO1A,GLG1,LCP1,PROS1,PTPRC,VCAN,WASF2

From the 54 significantly overrepresented proteins of antibody-mediated glomerular injuries compared to stable graft controls, protein association networks were analyzed using the online resource STRING v11.0. From the native results, this table presents the most relevant biological processes, according to the Gene Ontology terminology, while excluding redundancies for clarity. Native results are presented in Supplemental Table S2.

Table 4. Observed expression patterns of the WARS, TYMP, GBP1, CORO1A and EFHD2 antibodies in the analyzed kidney allograft biopsies

	Glomerular endothelial cells			Endothelial cells of peritubular capillary			Endothelial cells of arteries		Tubular cells			Inflammatory cells		Others
	SG	aABMR	Interstitial infiltrate	SG	aABMR	Interstitial infiltrate	SG	ABMR	SG	ABMR	Stress*	SG	ABMR	ABMR
WARS	+	++/+++	+	+	++/+++	++/+++	+	Variable	0	0	+	+	+/++	
TYMP	+/-	++	+/-	+/-	++/+++	++/+++	0	Variable	0	0	++ (atrophy)/+++	++	++/+++	+/++ glomerular epithelial cells
GBP1	0	+/++, focal	0	0	+/++, focal	+/++	0	Variable	0	0	+/++	+, scattered	+/++, scattered	
CORO1A	0	0	0	0	0	0	0	0	0	0	0	+++ (all)	+++ (all)	++ in some podocytes
EFHD2	0	0	0	0	0	0	0	0	0	0	0	+/++ (some**)	+/++ (some**)	

* stress refers to a tubulo-interstitial inflammation or acute tubular injury.

** EFHD2 stains some inflammatory cells with variable strength, no cell type predominance was morphologically seen.

Note that for CORO1A and EFHD2, staining intensity of inflammatory cells did not patently vary between ABMR and SG cases, relying on cell density to distinguish the entities.

Abbreviations: aABMR, active antibody-mediated rejection; SG, stable graft controls; WARS, tryptophan--tRNA ligase, cytoplasmic; TYMP, thymidine phosphorylase; GBP1, guanylate-binding protein 1, CORO1A, coronin-1A; EFHD2, EF-hand domain-containing protein D2.

Table 5. Diagnostic performances of the WARS, TYMP and GBP1 antibodies by immunohistochemistry for the diagnosis of aABMR in a selected cohort of kidney biopsies

	WARS			**TYMP**			**GBP1**		
	Sensitivity (%)	Specificity (%)	Cohen's kappa	Sensitivity (%)	Specificity (%)	Cohen's kappa	Sensitivity (%)	Specificity (%)	Cohen's kappa
Pathologist 1/BC	75	86	0,567	88	86	0,7	60	86	0,511
Pathologist 2/AV	69	84		75	89		67	89	

53 cases with 16 active ABMR cases (including 5 C4d positive) and 37 relevant differential diagnoses: T-cell mediated rejections (n=6), infections (3 polyomavirus nephropathies and 2 acute pyelonephritides), acute tubular injuries (n=5), recurrent or *de novo* glomerular nephropathies (3 IgA nephropathies and 2 membranous nephropathies), non-humoral thrombotic microangiopathies (n=5), isolated C4d positivity (n=3), chronic ABMR without activity (especially g0 cpt0, n=5) and stable graft cases in ABO incompatible transplantation (one year protocol biopsies without acute lesion, n=3).

Abbreviations: aABMR, active antibody-mediated rejection; WARS, tryptophan--tRNA ligase, cytoplasmic; TYMP, thymidine phosphorylase; GBP1, guanylate-binding protein 1.

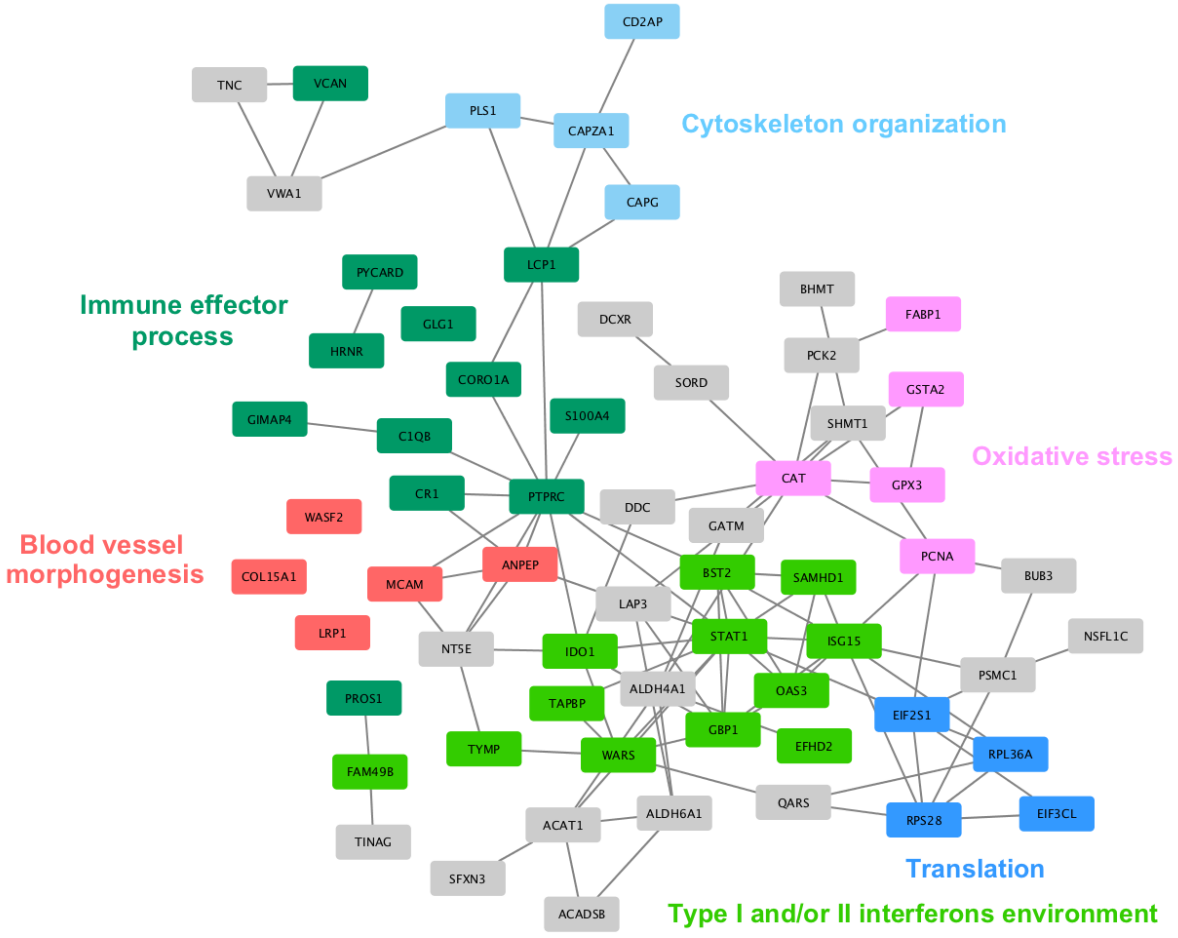

Figure 1. Integrative visual summary of the most relevant pathways involved in the 82 protein profile defining antibody-mediated glomerular injuries compared to stable graft controls. Each node represents a protein, defined by its corresponding gene name according to the UniProt database. Each line defines a physical and/or functional interaction between two proteins, as proposed by the online resource STRING v11. The graph was further adapted with Cytoscape version 3.7.1, to integrate other functional analyses, notably with the Ingenuity Pathway Analysis software. In this manner, nodes were labeled with a specific color to emphasize specific biological processes. All green nodes are immune-related, the light ones being more specifically part of the environment of the type I and II interferons. Note that the grey nodes are considered here by default, where no specific pathway is emphasized.

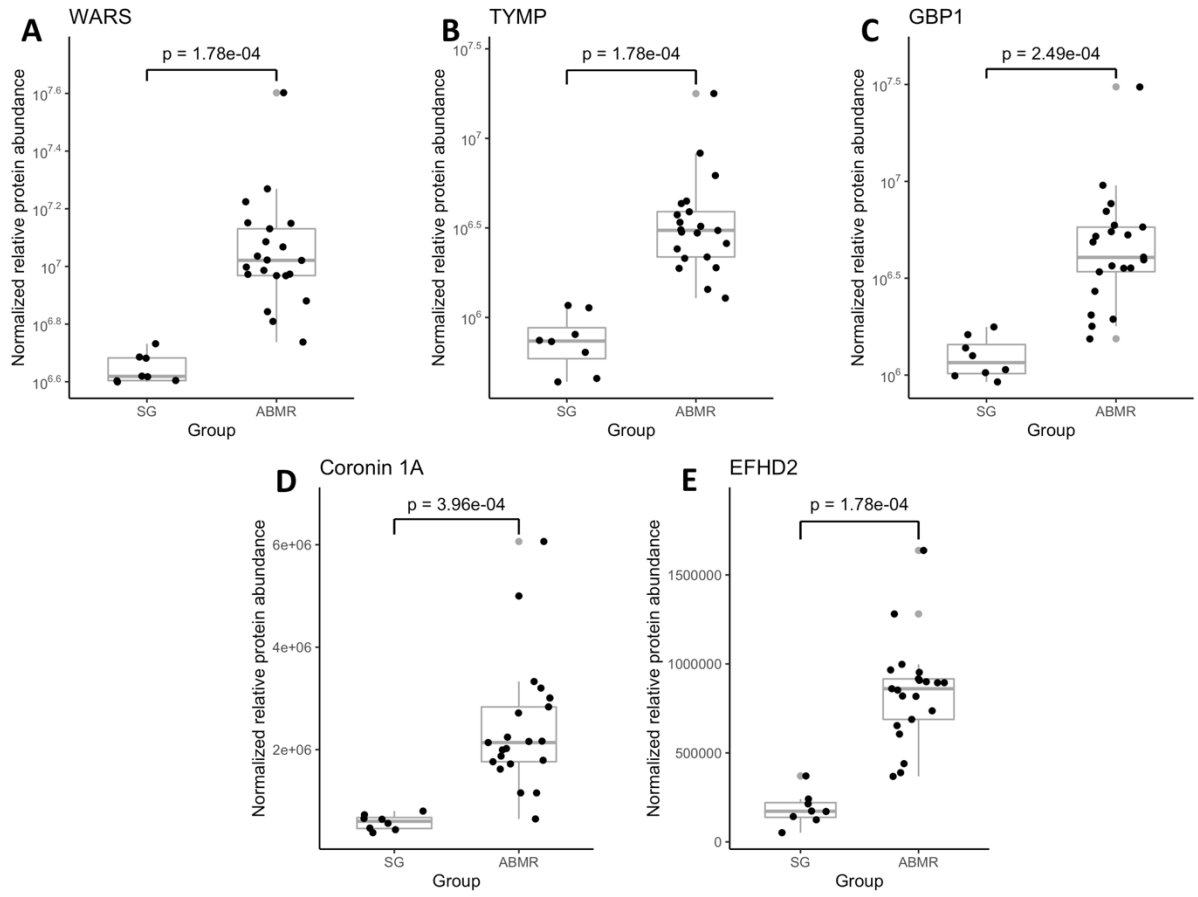

Figure 2. Relative protein abundance presented for all analyzed biopsies, as acquired by the mass spectrometer, depending on the group, for the proteins WARS (A), TYMP (B), GBP1 (C), CORO1A (D) and EFHD2 (E). An obvious overrepresentation of these five proteins in the active ABMR group compared to the stable graft one is present. Corresponding adjusted p-values are showed (Mann-Whitney test and Benjamini-Hochberg correction). ABMR, antibody-mediated rejection; SG, stable graft controls; WARS, tryptophan--tRNA ligase, cytoplasmic; TYMP, thymidine phosphorylase; GBP1, guanylate-binding protein 1; CORO1A, coronin-1A; EFHD2, EF-hand domain-containing protein D2.

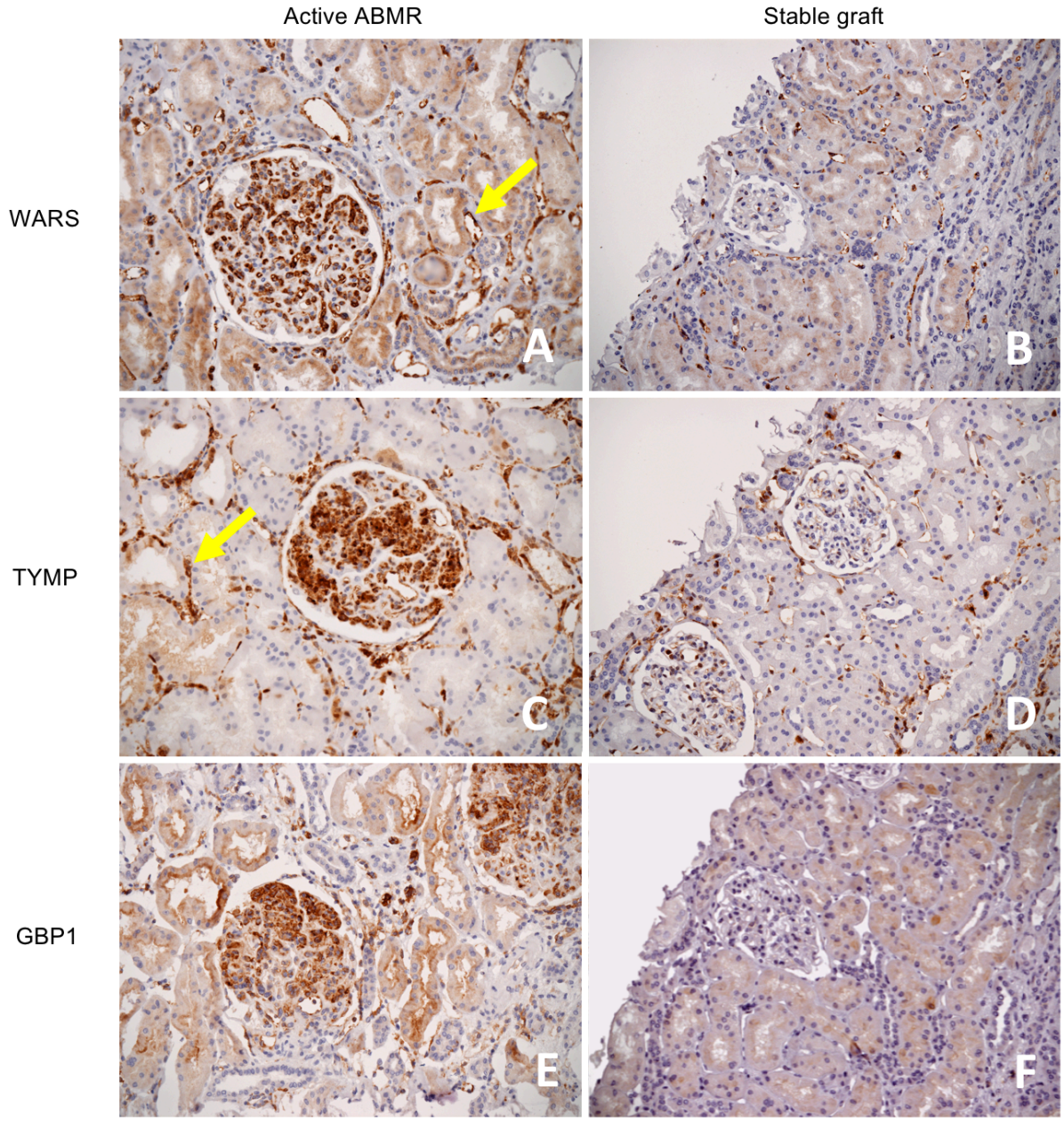

Figure 3. Immunohistochemical stainings for WARS, TYMP, GBP1, CORO1A and EFHD2 in an active antibody-mediated rejection (left) and a stable graft control case (right), original magnification x200. (A) shows a strong and diffuse cytoplasmic staining for WARS antibody on endothelial cells in active ABMR, both in the glomerulus and peritubular capillaries (arrow), compared to the stable graft control (B), where a weak constitutive staining exists. (C) shows a strong and diffuse staining for TYMP in endothelial and inflammatory cells, especially in the glomerulus but also in the peritubular capillaries (arrow). (D) Weak and focal staining for TYMP, predominantly in the peritubular capillary. (E) shows a strong staining for GBP1 in endothelial and inflammatory cells in the glomeruli. Within peritubular capillaries inflammatory cells are also strongly stained, whereas expression on endothelial cells is just focal and weak. Proximal tubular cells show a moderate staining predominant in the brush border. (F) No specific staining for GBP1 in a stable graft case.

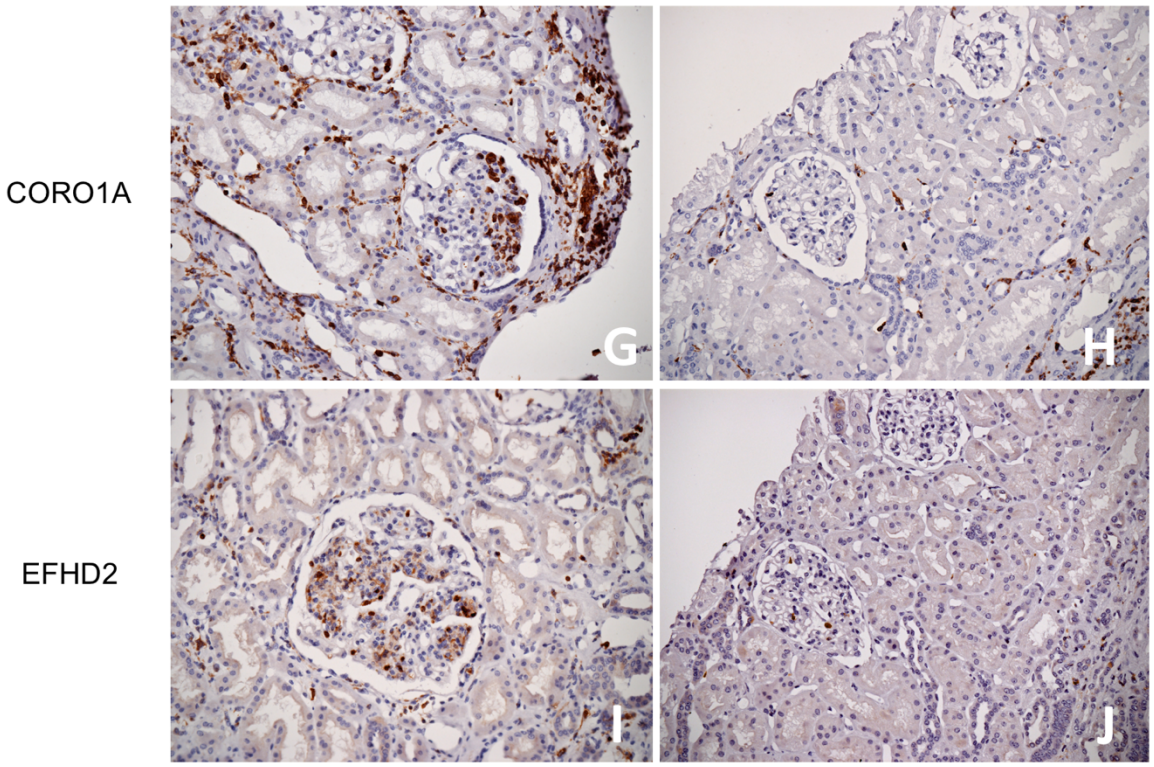

Figure 3. Immunohistochemical stainings for WARS, TYMP, GBP1, CORO1A and EFHD2 in an active antibody-mediated rejection (left) and a stable graft control case (right), original magnification x200 (continued). (G) shows a moderate to strong nuclear and cytoplasmic staining for EFHD2 antibody on some inflammatory cells in this active ABMR case, especially in the glomerulus but also in peritubular capillaries and in the interstitium. (H) shows a similar pattern of expression of EFHD2, but with globally much less positive cells. (I) shows a strong nuclear and cytoplasmic staining for CORO1A in noticeably all inflammatory cells, wherever they are. Many positive cells are visible in the glomerulus in this active ABMR case. (J) shows the same expression pattern of CORO1A, but limited to a few inflammatory cells in the peritubular capillaries or the interstitium.

E) Discussion

Antibody-mediated rejection remains a major issue in kidney transplantation. In this proof-of-concept study, we described the first glomerular proteome of aABMR from FFPE samples by combining microdissection with tandem mass spectrometry, and highlighted three interferon-related endothelial stress proteins, WARS, TYMP, GBP1, that showed good performances for the diagnosis of aABMR by immunohistochemistry with a moderate to strong reproducibility between two pathologists.

We described an 82 protein profile of active antibody-mediated glomerular injuries, overall mimicking an antiviral stress response. Indeed leukocyte activation is particularly highlighted through the overrepresentation of the interferons environment, both type I (SAMHD1, ISG15, OAS3, STAT1, BST2, VCAN) and II (STAT1, WARS, GBP1, TYMP, TAPBP, EFHD2, IDO1), in accordance with transcriptomic approaches (17,21). Of note EFDH2 is known to be involved in the translocation of a subunit of the interferon gamma (IFN-γ) receptor to the cell membrane of macrophages preceding their activation (48). The release of reactive oxygen species by macrophages through IFN-γ activation could then explain the described markers of oxidative stress (49). Cell adhesion and migration-involved proteins, notably through cytoskeleton reorganization, could also be considered as markers of leukocyte activation in the process of extravasation. In this setting, CORO1A is known to be involved in neutrophils trafficking in mice (50), and its deficiency was proved to suppress allo-specific T-cell response in skin and heart graft mouse models (51). Still in the adaptive response, the significant regulation of T-cell proliferation biological process indicates the involvement of T-cells during ABMR, as notably evidenced by a recent cellular infiltrate immunophenotyping study of ABMR cases (52). The identified translation knot, led by EIF2S1, which is deemed to be phosphorylated in this context by interferon gamma through PKR activation, participates in the antiviral response mimicking as part of the integrated stress response (53). Finally, the blood vessel morphogenesis pathway probably represents a remodeling of the microcirculation in the glomeruli, as an indirect witness of endothelial cells activation. In this setting, WARS is a well-known IFN-γ-induced protein, whose some fragments have described angiostatic effects, and thus is thought to play a role in vascular homeostasis (21,54,55). As for TYMP, it has both pro-angiogenic and pro-thrombotic effects (56), and was found to enhance C-X-C motif chemokine 10 (CXCL10) in an *in vitro* model of rheumatoid arthritis (57), a highly described cytokine in the context of ABMR (21,58). GBP1, also induced by IFN-γ in notably both endothelial cells and monocytes, globally inhibits cell proliferation and sensitivity to apoptosis and is crucial for the maturation of phagosomes for intracellular pathogens clearance (59,60).

The involvement of the complement system is only minor in our profile, despite at least 20 identified proteins (or fragments of proteins) of the complement system. This is possibly due to a minority of C4d positive cases in our cohort, even if the diagnostic peritubular capillaries positivity cannot let us think about predicting the whole complement status in the glomeruli, where a constitutive clearance of immune-complexes is also physiologically thought (61). We could however notice the

overrepresentation of a fragment of C1q, that could logically be recruited in this context by the bonded DSA, and the underrepresentation of CR1, which could in part explain a lack of inhibition of the C3 and C5 convertases leading to injuries (14).

As we are aware that without differential diagnoses analyzed by mass spectrometry, we cannot pretend to describe a specific profile of ABMR, our results still represent for now the most exhaustive description of the glomerular proteome modifications occurring in ABMR. Moreover, focusing on glomeruli allowed us to limit inter-samples proteome variability and restrict the analysis to the most specific morphological lesion of ABMR, for a more robust comparison from this small cohort. Finally, considering the aim of immunomarkers identification, we think that the *in situ* assessment of endothelial expression by immunohistochemistry studies allows pathologists to restore some specificity. This kind of cell-type expression analysis cannot be judged by molecular studies from a whole biopsy or even a multicellular microdissection. In this study we logically focused on endothelial cells expression for retaining an ABMR diagnosis. From the independent cohort, TYMP and WARS are for now the most promising antibodies, enabling a reasonable sensitivity as compared to C4d with still a good specificity. These two antibodies were in most cases easy to interpret, at a low-power field, with an inter-observer reproducibility strong to moderate respectively. GBP1 seemed less sensitive and reproducible, with mostly focal stainings on endothelial cells, despite good specificity. The positive criteria are dependent on the antibody, and will probably evolve as the experience of the pathologists will increase, to allow the best balance between reproducibility and performance for each antibody in the diagnosis of active ABMR. For now the most frequent false positive cases were some chronic ABMR deemed to be without activity (g0 cpt0) and some cases with severe tubulo-interstitial inflammation. The latter cases could often have been avoided by considering peritubular capillary staining nonspecific near these areas of severe tubulo-interstitial inflammation. As for the chronic ABMR cases, it could either represent true false positives, or evolving endothelial injuries without morphological microvascular inflammation, but in this latter case the prognostic impact and the value of a potential treatment are not currently defined. False negative cases were mainly due to stainings judged as either too focal and/or too weak.

Considering the limitations of our study, the proteomic analysis only concerned a small cohort of selected cases with no differential diagnosis other than stable graft controls for comparison. In the same way, the immunohistochemistry analysis of the selected immunomarkers of active ABMR was performed on a small retrospective cohort, though including relevant differential diagnoses. Moreover we must recognize that it is difficult for the pathologists to be truly blind to the diagnoses, considering the counterstaining that allows a partial morphological interpretation. But as already mentioned, most of the interpretations are made at low-power field (magnification x40 or x100) and thus this bias is limited. Finally, the thrombotic microangiopathy cases showed more chronic than acute features, that could have favored immunomarkers negativity.

To conclude, by focusing on the glomerular proteome in ABMR with anti-HLA DSA, this study brings the most exhaustive tissue proteic data in this disease to date, with evidences of a global cellular

stress mediated by the interferons, leukocyte activation, cell migration/adhesion and microcirculation remodeling processes. Three protein markers of endothelial stress through the interferons, TYMP, WARS and GBP1 have been isolated, that could represent relevant immunomarkers in the diagnosis of aABMR, as shown in an independent cohort of FFPE samples by immunohistochemistry. A prospective study of unselected cases seems crucial to evaluate the true benefits of these immunomarkers in this setting, as well as their potential prognostic value.

III- Perspectives

Ce travail illustre l'intérêt de l'analyse protéomique tissulaire par spectrométrie de masse dans la caractérisation physiopathologique d'entité lésionnelle ainsi que l'identification de potentiels biomarqueurs d'intérêt clinique. Dans cette étude pilote, nous nous sommes focalisés sur les modifications du protéome glomérulaire au cours du rejet humoral actif en transplantation rénale (glomérulite *versus* glomérule en conditions stables). Ainsi l'évolution du protéome observé traduit deux origines : (i) les protéines de la circulation, qu'elles soient introduites par des effecteurs cellulaires (cellules immunitaires ici) ou non (protéines du complément notamment) ; (ii) les modifications d'expression protéique générées par les cellules glomérulaires elles-mêmes (cellules endothéliales, mésangiales et épithéliales). Ce point est d'ailleurs souligné par le fait que les protéines testées en immunohistochimie sont toutes exprimées par une partie ou l'ensemble des cellules immunitaires, plus ou moins associé à un marquage des effecteurs cellulaires locaux (endothéliaux notamment). C'est ainsi que les protéines CORO1A et EFHD2 sont exprimées quasi-exclusivement par les cellules immunitaires, ce qui nous a conduit à les écarter dans cette étude pour le diagnostic de rejet humoral actif. Pour autant, leur quantification histologique à l'échelle glomérulaire présentait une excellente corrélation avec l'abondance relative proposée par le spectromètre de masse. Une valeur seuil était même définissable pour chaque anticorps afin de classer correctement l'ensemble des patients en « greffé stable » ou « rejet humoral actif » (données non présentées). Ceci ouvre la porte à une quantification plus objective des lésions de glomérulite et à une plus large exploration de la gamme dynamique d'intensité lésionnelle comparativement à celles du score semi-quantitatif « g » de la classification de Banff, actuellement gradé en 4 catégories (de 0 à 3) qui bénéficie seulement d'une reproductibilité faible (19,23). Pour autant, les impacts pronostique et thérapeutique de telles quantifications seraient respectivement à établir ou à déterminer.

Les trois autres protéines sélectionnées, WARS, GBP1 et TYMP, montrent, en sus du marquage des cellules immunitaires, une surexpression endothéliale au cours du rejet humoral et agissent ainsi comme des marqueurs de stress endothélial. Néanmoins celui-ci dépasse le cadre du mécanisme humoral, et des critères stricts doivent être employés pour associer le marquage à un mécanisme supposé humoral. A l'aide d'une première cohorte rétrospective de biopsies sélectionnées, nous avons montré

l'intérêt de ces 3 protéines en immunohistochimie pour un diagnostic de rejet humoral actif en transplantation rénale, potentiellement facilement transposable en routine. Une étude de plus grande envergure, prospective, sur des cas non sélectionnés, est maintenant nécessaire pour évaluer ces marqueurs en conditions cliniques réelles.

Bien que présentant des données très préliminaires, il faut également souligner la négativité, pour les 3 anticorps testés, des biopsies protocolaires de patients greffés stables en transplantation ABO incompatible. En effet, ces transplantations ABO incompatibles se traduisent par une activation constitutive de la voie classique du complément à la surface des cellules endothéliales par les anticorps naturels IgM du receveur. Pour autant, et sous réserve du protocole immunosuppresseur adapté, il s'y associe un mécanisme d'accommodation, se traduisant par l'absence d'altération cellulaire ou d'infiltrat inflammatoire associés à cette activation du complément, accompagnée d'un marquage constitutif intense et diffus du C4d à la surface des cellules endothéliales et *in fine* d'une préservation de la fonction du greffon (62). Ces mécanismes d'accommodation, surtout décrits en greffe ABO incompatible, ne sont que partiellement élucidés, mais impliquent notamment des effecteurs régulateurs du système du complément, notamment la surexpression des CD46 et CD59 membranaires (63). Ainsi, l'absence de surexpression observée pour WARS, GBP1 et TYMP dans ces cas de biopsies non inflammatoires en contexte ABO incompatible est un argument supplémentaire pour l'absence de stress endothélial dans ce contexte accommodatif. Ces marqueurs pourraient alors potentiellement se substituer au C4d comme critère de diagnostic histologique, rendu non contributif par sa positivité constitutive.

Une surexpression des transcrits de WARS et GBP1, induits par l'interféron gamma, a été retrouvée dans différentes transplantations d'organe solide, essentiellement cardiaque, et a été associée au mécanisme de rejet d'allogreffe (21). L'intérêt des protéines identifiées dans notre analyse protéique mériterait d'être testé sur d'autres transplantations d'organe, où des problématiques parfois similaires sont rencontrées, notamment dans le diagnostic du rejet humoral et la difficulté d'interprétation de l'immunomarquage C4d.

Par ailleurs, dans cette étude, l'analyse protéomique des glomérules par spectrométrie de masse permet de classer correctement les patients entre les groupes « rejet humoral » et « greffé stable », preuve d'une sensibilité technique suffisante malgré une très faible quantité de matériel biopsique FFPE analysée. Ceci soulève la question de son utilisation potentielle comme classificateur moléculaire tel que préconisé par la classification de Banff. La mise au point d'un tel classificateur nécessiterait l'analyse d'un plus grand nombre de cas, incluant les diagnostics différentiels principalement rencontrés en transplantation, afin de définir des signatures protéiques diagnostiques spécifiques de chaque entité lésionnelle. La pertinence clinique de tels classificateurs ne fait aucun doute et des recommandations sur les principales indications de telles analyses sont déjà avancées en transplantation rénale (7). Dans le même champ d'application, l'utilité de la protéomique par spectrométrie de masse dans l'analyse d'échantillons urinaires en transplantation rénale, déjà initiée par certaines équipes (34,64), mérite d'être évaluée, dans l'espoir futur d'un diagnostic non-invasif du rejet d'allogreffe.

Enfin, la caractérisation de profils protéiques par la protéomique tissulaire est un support physiopathologique d'intérêt. Là où les DSA ne semblent pas être les seuls responsables des lésions de la microcirculation (16), la MVI représente actuellement le point de convergence histologique de différents mécanismes d'agression immunologique du greffon : rejet humoral médié par des DSA anti-HLA (ici étudié), rejet humoral médié par des DSA non-HLA, rejet vasculaire médié par les cellules NK voire même autres mécanismes à découvrir. L'étude de ces différents phénotypes de rejet microvasculaire par spectrométrie de masse permettrait une meilleure caractérisation physiopathologique de ces différentes entités, et serait potentiellement à même d'ouvrir de nouvelles voies thérapeutiques, dans un domaine où les possibilités actuelles de traitement sont limitées.

IV- Références

1. Agence de biomédecine. Rapport médical et scientifique 2018 [Internet]. 2019 sept. Disponible sur: https://rams.agence-biomedecine.fr/greffe-renale

2. Sellarés J, de Freitas DG, Mengel M, Reeve J, Einecke G, Sis B, et al. Understanding the causes of kidney transplant failure: the dominant role of antibody-mediated rejection and nonadherence. Am J Transplant. févr 2012;12(2):388-99.

3. Cooper JE. Evaluation and Treatment of Acute Rejection in Kidney Allografts. Clin J Am Soc Nephrol. 06 2020;15(3):430-8.

4. Loupy A, Lefaucheur C. Antibody-Mediated Rejection of Solid-Organ Allografts. N Engl J Med. 20 2018;379(12):1150-60.

5. Naesens M, Kuypers DRJ, De Vusser K, Evenepoel P, Claes K, Bammens B, et al. The histology of kidney transplant failure: a long-term follow-up study. Transplantation. 27 août 2014;98(4):427-35.

6. Colvin RB, Smith RN. Antibody-mediated organ-allograft rejection. Nat Rev Immunol. oct 2005;5(10):807-17.

7. Haas M. Evolving criteria for the diagnosis of antibody-mediated rejection in renal allografts. Curr Opin Nephrol Hypertens. 2018;27(3):137-43.

8. Gloor J, Stegall MD. Sensitized renal transplant recipients: current protocols and future directions. Nat Rev Nephrol. mai 2010;6(5):297-306.

9. Gloor JM, Sethi S, Stegall MD, Park WD, Moore SB, DeGoey S, et al. Transplant glomerulopathy: subclinical incidence and association with alloantibody. Am J Transplant. sept 2007;7(9):2124-32.

10. Delville M, Lamarthée B, Pagie S, See SB, Rabant M, Burger C, et al. Early Acute Microvascular Kidney Transplant Rejection in the Absence of Anti-HLA Antibodies Is Associated with Preformed IgG Antibodies against Diverse Glomerular Endothelial Cell Antigens. J Am Soc Nephrol. avr 2019;30(4):692-709.

11. Aubert O, Loupy A, Hidalgo L, Duong van Huyen J-P, Higgins S, Viglietti D, et al. Antibody-Mediated Rejection Due to Preexisting versus De Novo Donor-Specific Antibodies in Kidney Allograft Recipients. J Am Soc Nephrol. juin 2017;28(6):1912-23.

12. Liszewski MK, Farries TC, Lublin DM, Rooney IA, Atkinson JP. Control of the complement system. Adv Immunol. 1996;61:201-83.

13. Racusen LC, Colvin RB, Solez K, Mihatsch MJ, Halloran PF, Campbell PM, et al. Antibody-mediated rejection criteria - an addition to the Banff 97 classification of renal allograft rejection. Am J Transplant. juin 2003;3(6):708-14.

14. Biglarnia A-R, Huber-Lang M, Mohlin C, Ekdahl KN, Nilsson B. The multifaceted role of complement in kidney transplantation. Nat Rev Nephrol. 2018;14(12):767-81.

15. Sis B, Jhangri GS, Bunnag S, Allanach K, Kaplan B, Halloran PF. Endothelial gene expression in kidney transplants with alloantibody indicates antibody-mediated damage despite lack of C4d staining. Am J Transplant. oct 2009;9(10):2312-23.

16. Koenig A, Chen C-C, Marçais A, Barba T, Mathias V, Sicard A, et al. Missing self triggers NK cell-mediated chronic vascular rejection of solid organ transplants. Nat Commun. 25 nov 2019;10(1):5350.

17. Sis B, Halloran PF. Endothelial transcripts uncover a previously unknown phenotype: C4d-negative antibody-mediated rejection. Curr Opin Organ Transplant. févr 2010;15(1):42-8.

18. Loupy A, Haas M, Roufosse C, Naesens M, Adam B, Afrouzian M, et al. The Banff 2019 Kidney Meeting Report (I): Updates on and clarification of criteria for T cell– and antibody-mediated rejection. Am J Transplant. mai 2020;00:1-14.

19. Haas M, Sis B, Racusen LC, Solez K, Glotz D, Colvin RB, et al. Banff 2013 meeting report: inclusion of c4d-negative antibody-mediated rejection and antibody-associated arterial lesions. Am J Transplant. févr 2014;14(2):272-83.

20. Gibson IW, Gwinner W, Bröcker V, Sis B, Riopel J, Roberts ISD, et al. Peritubular capillaritis in renal allografts: prevalence, scoring system, reproducibility and clinicopathological correlates. Am J Transplant. avr 2008;8(4):819-25.

21. Halloran PF, Venner JM, Madill-Thomsen KS, Einecke G, Parkes MD, Hidalgo LG, et al. Review: The transcripts associated with organ allograft rejection. Am J Transplant. avr 2018;18(4):785-95.

22. Halloran PF, Reeve J, Akalin E, Aubert O, Bohmig GA, Brennan D, et al. Real Time Central Assessment of Kidney Transplant Indication Biopsies by Microarrays: The INTERCOMEX Study. Am J Transplant. 27 avr 2017;

23. Haas M, Loupy A, Lefaucheur C, Roufosse C, Glotz D, Seron D, et al. The Banff 2017 Kidney Meeting Report: Revised diagnostic criteria for chronic active T cell-mediated rejection, antibody-mediated rejection, and prospects for integrative endpoints for next-generation clinical trials. Am J Transplant. févr 2018;18(2):293-307.

24. Adam BA, Smith RN, Rosales IA, Matsunami M, Afzali B, Oura T, et al. Chronic Antibody-Mediated Rejection in Nonhuman Primate Renal Allografts: Validation of Human Histological and Molecular Phenotypes. Am J Transplant. nov 2017;17(11):2841-50.

25. Mengel M, Loupy A, Haas M, Roufosse C, Naesens M, Akalin E, et al. Banff 2019 Meeting Report: Molecular diagnostics in solid organ transplantation-Consensus for the Banff Human Organ Transplant (B-HOT) gene panel and open source multicenter validation. Am J Transplant. 19 mai 2020;

26. Gwinner W, Metzger J, Husi H, Marx D. Proteomics for rejection diagnosis in renal transplant patients: Where are we now? World J Transplant. 24 mars 2016;6(1):28-41.

27. Vogel C, Marcotte EM. Insights into the regulation of protein abundance from proteomic and transcriptomic analyses. Nat Rev Genet. 13 mars 2012;13(4):227-32.

28. Addis MF, Tanca A, Pagnozzi D, Crobu S, Fanciulli G, Cossu-Rocca P, et al. Generation of high-quality protein extracts from formalin-fixed, paraffin-embedded tissues. Proteomics. août 2009;9(15):3815-23.

29. Henriet E, Hammoud AA, Dupuy J-W, Dartigues B, Ezzoukry Z, Dugot-Senant N, et al. Argininosuccinate synthase 1 (ASS1): A marker of unclassified hepatocellular adenoma and high bleeding risk. Hepatology. 23 juin 2017;

30. Haas M. Glomerular Disease Pathology in the Era of Proteomics: From Pattern to Pathogenesis. J Am Soc Nephrol. janv 2018;29(1):2-4.

31. Andeen NK, Yang H-Y, Dai D-F, MacCoss MJ, Smith KD. DnaJ Homolog Subfamily B Member 9 Is a Putative Autoantigen in Fibrillary GN. J Am Soc Nephrol. janv 2018;29(1):231-9.

32. Nasr SH, Vrana JA, Dasari S, Bridoux F, Fidler ME, Kaaki S, et al. DNAJB9 Is a Specific Immunohistochemical Marker for Fibrillary Glomerulonephritis. Kidney Int Rep. janv 2018;3(1):56-64.

33. Sethi S, Madden BJ, Debiec H, Charlesworth MC, Gross L, Ravindran A, et al. Exostosin 1/Exostosin 2-Associated Membranous Nephropathy. J Am Soc Nephrol. juin 2019;30(6):1123-36.

34. Sigdel TK, Gao Y, He J, Wang A, Nicora CD, Fillmore TL, et al. Mining the human urine proteome for monitoring renal transplant injury. Kidney Int. 2016;89(6):1244-52.

35. Lin X-C, Sui W-G, Qi S-W, Tang D-E, Cong S, Zou G-M, et al. Quantitative proteomic profiling of renal tissue in human chronic rejection biopsy samples after renal transplantation. Transplant Proc. mars 2015;47(2):323-31.

36. Nakorchevsky A, Hewel JA, Kurian SM, Mondala TS, Campbell D, Head SR, et al. Molecular mechanisms of chronic kidney transplant rejection via large-scale proteogenomic analysis of tissue biopsies. J Am Soc Nephrol. févr 2010;21(2):362-73.

37. Lamb KE, Lodhi S, Meier-Kriesche H-U. Long-term renal allograft survival in the United States: a critical reappraisal. Am J Transplant. mars 2011;11(3):450-62.

38. Loupy A, Haas M, Solez K, Racusen L, Glotz D, Seron D, et al. The Banff 2015 Kidney Meeting Report: Current Challenges in Rejection Classification and Prospects for Adopting Molecular Pathology. Am J Transplant. janv 2017;17(1):28-41.

39. Venner JM, Hidalgo LG, Famulski KS, Chang J, Halloran PF. The molecular landscape of antibody-mediated kidney transplant rejection: evidence for NK involvement through CD16a Fc receptors. Am J Transplant. mai 2015;15(5):1336-48.

40. Sellarés J, Reeve J, Loupy A, Mengel M, Sis B, Skene A, et al. Molecular diagnosis of antibody-mediated rejection in human kidney transplants. Am J Transplant. avr 2013;13(4):971-83.

41. Ezzoukhry Z, Henriet E, Cordelières FP, Dupuy J-W, Maître M, Gay N, et al. Combining laser capture microdissection and proteomics reveals an active translation machinery controlling invadosome formation. Nat Commun. 23 2018;9(1):2031.

42. Dasari S, Alexander MP, Vrana JA, Theis JD, Mills JR, Negron V, et al. DnaJ Heat Shock Protein Family B Member 9 Is a Novel Biomarker for Fibrillary GN. J Am Soc Nephrol. janv 2018;29(1):51-6.

43. Bouyssié D, Hesse A-M, Mouton-Barbosa E, Rompais M, Macron C, Carapito C, et al. Proline: an efficient and user-friendly software suite for large-scale proteomics. Bioinformatics. 1 mai 2020;36(10):3148-55.

44. Benjamini Y, Hochberg Y. Controlling The False Discovery Rate - A Practical And Powerful Approach To Multiple Testing. J Royal Statist Soc, Series B. 30 nov 1995;57:289-300.

45. Szklarczyk D, Gable AL, Lyon D, Junge A, Wyder S, Huerta-Cepas J, et al. STRING v11: protein-protein association networks with increased coverage, supporting functional discovery in genome-wide experimental datasets. Nucleic Acids Res. 8 janv 2019;47(D1):D607-13.

46. Liaw A, Wiener M. Classification and Regression by randomForest. R News. 2002;2(3):18--22.

47. R Core Team. R: A Language and Environment for Statistical Computing [Internet]. R Foundation for Statistical Computing; 2019. Disponible sur: https://www.R-project.org

48. Xu X, Xu J, Wu J, Hu Y, Han Y, Gu Y, et al. Phosphorylation-Mediated IFN-γR2 Membrane Translocation Is Required to Activate Macrophage Innate Response. Cell. 15 2018;175(5):1336-1351.e17.

49. Lee AJ, Ashkar AA. The Dual Nature of Type I and Type II Interferons. Front Immunol. 2018;9:2061.

50. Pick R, Begandt D, Stocker TJ, Salvermoser M, Thome S, Böttcher RT, et al. Coronin 1A, a novel player in integrin biology, controls neutrophil trafficking in innate immunity. Blood. 17 2017;130(7):847-58.

51. Jayachandran R, Gumienny A, Bolinger B, Ruehl S, Lang MJ, Fucile G, et al. Disruption of Coronin 1 Signaling in T Cells Promotes Allograft Tolerance while Maintaining Anti-Pathogen Immunity. Immunity. 15 2019;50(1):152-165.e8.

52. Calvani J, Terada M, Lesaffre C, Eloudzeri M, Lamarthée B, Burger C, et al. In situ multiplex immunofluorescence analysis of the inflammatory burden in kidney allograft rejection: A new tool to characterize the alloimmune response. Am J Transplant. avr 2020;20(4):942-53.

53. Pakos-Zebrucka K, Koryga I, Mnich K, Ljujic M, Samali A, Gorman AM. The integrated stress response. EMBO Rep. 2016;17(10):1374-95.

54. Tzima E, Reader JS, Irani-Tehrani M, Ewalt KL, Schwartz MA, Schimmel P. Biologically active fragment of a human tRNA synthetase inhibits fluid shear stress-activated responses of endothelial cells. Proc Natl Acad Sci USA. 9 déc 2003;100(25):14903-7.

55. Wakasugi K, Slike BM, Hood J, Otani A, Ewalt KL, Friedlander M, et al. A human aminoacyl-tRNA synthetase as a regulator of angiogenesis. Proc Natl Acad Sci USA. 8 janv 2002;99(1):173-7.

56. Li W, Yue H. Thymidine phosphorylase: A potential new target for treating cardiovascular disease. Trends Cardiovasc Med. 2018;28(3):157-71.

57. Toyoda Y, Tabata S, Kishi J, Kuramoto T, Mitsuhashi A, Saijo A, et al. Thymidine phosphorylase regulates the expression of CXCL10 in rheumatoid arthritis fibroblast-like synoviocytes. Arthritis & Rheumatology (Hoboken, NJ). mars 2014;66(3):560-8.

58. Rabant M, Amrouche L, Lebreton X, Aulagnon F, Benon A, Sauvaget V, et al. Urinary C-X-C Motif Chemokine 10 Independently Improves the Noninvasive Diagnosis of Antibody-Mediated Kidney Allograft Rejection. J Am Soc Nephrol. nov 2015;26(11):2840-51.

59. Honkala AT, Tailor D, Malhotra SV. Guanylate-Binding Protein 1: An Emerging Target in Inflammation and Cancer. Front Immunol. 2019;10:3139.

60. Naschberger E, Bauer M, Stürzl M. Human guanylate binding protein-1 (hGBP-1) characterizes and establishes a non-angiogenic endothelial cell activation phenotype in inflammatory diseases. Adv Enzyme Regul. 2005;45:215-27.

61. Zwirner J, Felber E, Herzog V, Riethmüller G, Feucht HE. Classical pathway of complement activation in normal and diseased human glomeruli. Kidney Int. déc 1989;36(6):1069-77.

62. Garcia de Mattos Barbosa M, Cascalho M, Platt JL. Accommodation in ABO-incompatible organ transplants. Xenotransplantation. 2018;25(3):e12418.

63. Hruba P, Krejcik Z, Stranecky V, Maluskova J, Slatinska J, Gueler F, et al. Molecular Patterns Discriminate Accommodation and Subclinical Antibody-mediated Rejection in Kidney Transplantation. Transplantation. 2019;103(5):909-17.

64. Kanzelmeyer NK, Zürbig P, Mischak H, Metzger J, Fichtner A, Ruszai KH, et al. Urinary proteomics to diagnose chronic active antibody-mediated rejection in pediatric kidney transplantation - a pilot study. Transpl Int. 25 oct 2018;

V- Annexes : Supplemental Material

TABLE OF CONTENTS

Supplemental Table S1. List of the 82 proteins differentiating active antibody-mediated glomerular injuries from stable grafts, in ascending order of adjusted p-values

UniProt access	Full protein name	Corresponding gene name	Ratio of medians aABMR/SG	Adjusted p-values
P19971	Thymidine phosphorylase	TYMP	4.15	1.78E-04
Q96C19	EF-hand domain-containing protein D2	EFHD2	5.00	1.78E-04
P23381	Tryptophan--tRNA ligase, cytoplasmic	WARS	2.53	1.78E-04
Q9UJW2	Tubulointerstitial nephritis antigen	TINAG	0.35	1.78E-04
P32455	Guanylate-binding protein 1	GBP1	3.48	2.49E-04
P31146	Coronin-1A	CORO1A	3.56	3.96E-04
Q9ULZ3	Apoptosis-associated speck-like protein containing a CARD	PYCARD	18.78	4.98E-04
P13796	Plastin-2	LCP1	3.90	4.98E-04
A0A087X1J7	Glutathione peroxidase	GPX3	0.43	9.82E-04
P50440	Glycine amidinotransferase, mitochondrial	GATM	0.31	2.21E-03
Q13596	Sorting nexin-1	SNX1	2.04	2.82E-03
P09210	Glutathione S-transferase A2	GSTA2	0.31	2.82E-03
E9PF17	Versican core protein	VCAN	13.57	3.16E-03
P28838	Cytosol aminopeptidase	LAP3	2.01	3.16E-03
P42224	Signal transducer and activator of transcription 1-alpha/beta	STAT1	3.04	3.16E-03
Q9Y3Z3	Deoxynucleoside triphosphate triphosphohydrolase SAMHD1	SAMHD1	2.26	3.16E-03
P52907	F-actin-capping protein subunit alpha-1	CAPZA1	2.11	3.16E-03
P04040	Catalase	CAT	0.48	3.16E-03
H3BM42	Golgi apparatus protein 1, isoform CRA_c	GLG1	9.44	3.91E-03
P43121	Cell surface glycoprotein MUC18	MCAM	2.26	3.91E-03
P17927	Complement receptor type 1	CR1	0.39	3.91E-03
H7C0J5	Centrosomal protein of 104 kDa	CEP104	0.46	3.91E-03
G5E9W9	GTPase IMAP family member 4	GIMAP4	2.24	4.80E-03
A0A0A0MS41	Sideroflexin	SFXN3	7.27	4.80E-03
J3QT28	Mitotic checkpoint protein BUB3 (Fragment)	BUB3	6.40	6.00E-03
E9PHS0	Glutathione S-transferase LANCL1 (Fragment)	LANCL1	3.11	6.76E-03
Q93088	Betaine--homocysteine S-methyltransferase 1	BHMT	0.48	7.98E-03
Q6IB77	Glycine N-acyltransferase	GLYAT	0.37	7.98E-03
Q16822	Phosphoenolpyruvate carboxykinase [GTP], mitochondrial	PCK2	0.33	7.98E-03
A0A1B0GVU9	Glutamine--tRNA ligase (Fragment)	QARS	2.00	9.11E-03
A0A0U1RQV3	EGF-containing fibulin-like extracellular matrix protein 1 (Fragment)	EFEMP1	2.60	9.11E-03
Q96DG6	Carboxymethylenebutenolidase homolog	CMBL	0.43	9.11E-03
O76041	Nebulette	NEBL	0.35	1.05E-02
Q9BQI0	Allograft inflammatory factor 1-like	AIF1L	0.48	1.05E-02
P30039	Phenazine biosynthesis-like domain-containing protein	PBLD	0.46	1.05E-02
P05198	Eukaryotic translation initiation factor 2 subunit 1	EIF2S1	4.36	1.22E-02
P62857	40S ribosomal protein S28	RPS28	15.59	1.22E-02
P14902	Indoleamine 2,3-dioxygenase 1	IDO1	2.52	1.22E-02
P12004	Proliferating cell nuclear antigen	PCNA	2.83	1.22E-02
Q02252	Methylmalonate-semialdehyde dehydrogenase [acylating], mitochondrial	ALDH6A1	0.32	1.22E-02
A0A0A0MSV9	Tapasin	TAPBP	3.26	1.45E-02
A0A075B788	Receptor-type tyrosine-protein phosphatase C	PTPRC	8.96	1.45E-02
Q14651	Plastin-1	PLS1	2.68	1.45E-02
P26447	Protein S100-A4	S100A4	2.54	1.65E-02
Q13185	Chromobox protein homolog 3	CBX3	5.44	1.65E-02
A8MW49	Fatty acid-binding protein, liver	FABP1	0.40	1.65E-02
P30038	Delta-1-pyrroline-5-carboxylate dehydrogenase, mitochondrial	ALDH4A1	0.42	1.65E-02
Q9Y6K5	2'-5'-oligoadenylate synthase 3	OAS3	4.81	1.91E-02
Q9Y6W5	Wiskott-Aldrich syndrome protein family member 2	WASF2	3.07	1.91E-02
J3KS22	L-xylulose reductase (Fragment)	DCXR	0.45	1.91E-02
Q96CX2	BTB/POZ domain-containing protein KCTD12	KCTD12	2.45	2.14E-02
P21589	5'-nucleotidase	NT5E	2.87	2.14E-02
P24752	Acetyl-CoA acetyltransferase, mitochondrial	ACAT1	0.47	2.14E-02
Q86YZ3	Hornerin	HRNR	0.40	2.14E-02
H0Y5B4	60S ribosomal protein L36a	RPL36A	3.44	2.40E-02
J3QSU6	Tenascin	TNC	2.06	2.40E-02
Q07954	Prolow-density lipoprotein receptor-related protein 1	LRP1	4.02	2.40E-02
Q10589	Bone marrow stromal antigen 2	BST2	3.15	2.40E-02
Q9Y5K6	CD2-associated protein	CD2AP	5.95	2.40E-02
A0A087WV24	Aromatic-L-amino-acid decarboxylase	DDC	0.49	2.40E-02
P45954	Short/branched chain specific acyl-CoA dehydrogenase, mitochondrial	ACADSB	0.28	2.40E-02
B5ME19	Eukaryotic translation initiation factor 3 subunit C-like protein	EIF3CL	2.16	2.73E-02
Q9UJY1	Heat shock protein beta-8	HSPB8	3.45	2.73E-02
B0QYK4	EMI domain-containing protein 1	EMID1	3.32	2.73E-02

Q9BVM4	Gamma-glutamylaminecyclotransferase	GGACT	0.45	2.73E-02
P35527	Keratin, type I cytoskeletal 9	KRT9	0.43	2.73E-02
P62191	26S proteasome regulatory subunit 4	PSMC1	2.47	2.86E-02
A0A096LNZ9	Ubiquitin-like protein ISG15 (Fragment)	ISG15	3.75	2.86E-02
P34896	Serine hydroxymethyltransferase, cytosolic	SHMT1	0.44	2.86E-02
A0A0S2Z4L3	Protein S isoform 2 (Fragment)	PROS1	5.49	3.13E-02
A0A0A0MSV6	Complement C1q subcomponent subunit B (Fragment)	C1QB	2.55	3.13E-02
E5RI16	Protein FAM49B (Fragment)	FAM49B	5.74	3.13E-02
P15144	Aminopeptidase N	ANPEP	0.48	3.13E-02
Q6PCB0	von Willebrand factor A domain-containing protein 1	VWA1	3.39	3.45E-02
B7Z5J4	Carboxypeptidase A4	CPA4	2.31	3.45E-02
P40121	Macrophage-capping protein	CAPG	4.64	3.45E-02
A0A2R8Y7G9	Uncharacterized protein	H3,Y	2.87	3.45E-02
Q9UNZ2	NSFL1 cofactor p47	NSFL1C	2.04	3.45E-02
A0A087X0K0	Collagen alpha-1(XV) chain	COL15A1	2.52	4.20E-02
Q9NR31	GTP-binding protein SAR1a	SAR1A	3.87	4.20E-02
P02730	Band 3 anion transport protein	SLC4A1	0.34	4.20E-02
Q00796	Sorbitol dehydrogenase	SORD	0.50	4.77E-02

Non-parametric Mann-Whitney tests were performed to compare the protein expressions between the active antibody-mediated rejection (aABMR) and stable graft (SG) group. P-values were secondarily adjusted according to the Benjamini-Hochberg correction. A fold change aABMR/SG above 2 implies a significant overrepresentation of the protein in the lesional group, whereas a fold change below 0.5 an underrepresentation. Abbreviations: aABMR, active antibody-mediated rejection; SG, stable graft control.

Supplemental Table S2. Top-50 biological processes (GO terminology) from the 54 significantly overrepresented proteins of antibody-mediated glomerular injuries compared to stable graft controls, according to the online resource STRING v11.0, in ascending order of false discovery rate

GO-term	Term description	Observed protein count	Background protein count	False discovery rate	Involved proteins (labels)
GO:0051607	defense response to virus	8	181	8.35e-05	BST2,GBP1,ISG15,OAS3,PTPRC,PYCARD,SAMHD1,STAT1
GO:0002252	immune effector process	13	927	0.00080	BST2,C1QB,CORO1A,GBP1,ISG15,LCP1,LRP1,OAS3,PTPRC,PYCARD,SAMHD1,STAT1,WASF2
GO:0032956	regulation of actin cytoskeleton organization	8	297	0.00080	BST2,CAPG,CAPZA1,CD2AP,CORO1A,LRP1,PYCARD,WASF2
GO:0048519	negative regulation of biological process	30	4953	0.00080	BST2,BUB3,CAPG,CAPZA1,CBX3,CD2AP,CDYL,CORO1A,EFEMP1,EIF2S1,GBP1,GLG1,IDO1,ISG15,LRP1,NSFL1C,NT5E,OAS3,PCNA,PROS1,PSMC1,PTPRC,PYCARD,QARS,RPL36A,RPS28,STAT1,TNC,WARS,WASF2
GO:0060337	type I interferon signaling pathway	5	65	0.00080	BST2,ISG15,OAS3,SAMHD1,STAT1
GO:0051493	regulation of cytoskeleton organization	9	477	0.0012	BST2,CAPG,CAPZA1,CD2AP,CORO1A,LRP1,NSFL1C,PYCARD,WASF2
GO:0045087	innate immune response	10	676	0.0025	BST2,C1QB,CAPZA1,CORO1A,GBP1,ISG15,OAS3,PYCARD,SAMHD1,STAT1
GO:0006952	defense response	13	1234	0.0036	BST2,C1QB,CAPZA1,CORO1A,GBP1,IDO1,ISG15,LRP1,OAS3,PTPRC,PYCARD,SAMHD1,STAT1
GO:0050776	regulation of immune response	11	873	0.0036	BST2,C1QB,FAM49B,GBP1,IDO1,PROS1,PTPRC,PYCARD,SAMHD1,STAT1,WASF2
GO:0002376	immune system process	18	2370	0.0050	BST2,C1QB,CAPZA1,CORO1A,GBP1,GLG1,IDO1,ISG15,LCP1,LRP1,OAS3,PROS1,PTPRC,PYCARD,SAMHD1,STAT1,TAPBP,WASF2
GO:0001818	negative regulation of cytokine production	6	245	0.0073	BST2,CD2AP,GBP1,IDO1,ISG15,PYCARD
GO:0006955	immune response	14	1560	0.0073	BST2,C1QB,CAPZA1,CORO1A,GBP1,ISG15,LCP1,LRP1,OAS3,PTPRC,PYCARD,SAMHD1,STAT1,TAPBP
GO:0019221	cytokine-mediated signaling pathway	9	655	0.0076	BST2,CAPZA1,GBP1,ISG15,LCP1,OAS3,PYCARD,SAMHD1,STAT1
GO:0002682	regulation of immune system process	13	1391	0.0082	BST2,C1QB,CORO1A,FAM49B,GBP1,IDO1,ISG15,PROS1,PTPRC,PYCARD,SAMHD1,STAT1,WASF2
GO:0032269	negative regulation of cellular protein metabolic process	11	1014	0.0083	BST2,CDYL,EIF2S1,GBP1,GLG1,ISG15,PROS1,PTPRC,PYCARD,QARS,WARS
GO:0048523	negative regulation of cellular process	25	4454	0.0105	BST2,BUB3,CAPG,CAPZA1,CBX3,CD2AP,CDYL,CORO1A,EFEMP1,EIF2S1,GBP1,GLG1,IDO1,ISG15,LRP1,PCNA,PROS1,PSMC1,PTPRC,PYCARD,QARS,STAT1,TNC,WARS,WASF2
GO:0048525	negative regulation of viral process	4	93	0.0122	BST2,ISG15,OAS3,STAT1
GO:0043254	regulation of protein complex assembly	7	425	0.0132	CAPG,CAPZA1,CORO1A,LCP1,PSMC1,PYCARD,WARS
GO:0072673	lamellipodium morphogenesis	2	6	0.0151	SNX1,WASF2
GO:0071345	cellular response to cytokine stimulus	10	953	0.0182	BST2,CAPZA1,CORO1A,GBP1,ISG15,LCP1,OAS3,PYCARD,SAMHD1,STAT1
GO:0001817	regulation of cytokine production	8	615	0.0183	BST2,CD2AP,FAM49B,GBP1,IDO1,ISG15,PYCARD,STAT1
GO:0006950	response to stress	20	3267	0.0183	BST2,C1QB,CAPZA1,CORO1A,EIF2S1,GBP1,IDO1,ISG15,LRP1,MCAM,OAS3,PCNA,PROS1,PSMC1,PTPRC,PYCARD,SAMHD1,STAT1,TNC,VWA1
GO:0033043	regulation of organelle organization	11	1155	0.0183	BST2,BUB3,CAPG,CAPZA1,CD2AP,CORO1A,LCP1,LRP1,NSFL1C,PYCARD,WASF2
GO:1901564	organonitrogen compound metabolic process	27	5281	0.0183	BUB3,C1QB,CD2AP,CPA4,EFEMP1,EIF2S1,EIF3CL,IDO1,ISG15,LAP3,LRP1,NSFL1C,NT5E,PCNA,PSMC1,PTPRC,PYCARD,QARS,RPL36A,RPS28,SAMHD1,TAPBP,TNC,TYMP,VCAN,VWA1,WARS
GO:1901565	organonitrogen compound catabolic process	10	958	0.0183	BUB3,CD2AP,IDO1,ISG15,NSFL1C,NT5E,PSMC1,SAMHD1,TYMP,VCAN

GO:1902904	negative regulation of supramolecular fiber organization	4	115	0.0185	CAPG,CAPZA1,CORO1A,WASF2
GO:0050789	regulation of biological process	43	11116	0.0212	BST2,BUB3,C1QB,CAPG,CAPZA1,CBX3,CD2AP,CDYL,COL15A1,CORO1A,EFEMP1,EIF2S1,FAM49B,GBP1,GLG1,HSPB8,IDO1,ISG15,LANCL1,LCP1,LRP1,MCAM,NSFL1C,NT5E,OAS3,PCNA,PLS1,PROS1,PSMC1,PTPRC,PYCARD,QARS,RPL36A,RPS28,S100A4,SAMHD1,SNX1,STAT1,TAPBP,TNC,TYMP,WARS,WASF2
GO:0051494	negative regulation of cytoskeleton organization	4	121	0.0212	CAPG,CAPZA1,CORO1A,WASF2
GO:0009605	response to external stimulus	14	1857	0.0214	BST2,CORO1A,EIF2S1,GBP1,IDO1,ISG15,OAS3,PCNA,PTPRC,PYCARD,SAMHD1,STAT1,TNC,TYMP
GO:0002697	regulation of immune effector process	6	362	0.0225	BST2,C1QB,FAM49B,PROS1,PTPRC,STAT1
GO:0006412	translation	6	362	0.0225	EIF2S1,EIF3CL,QARS,RPL36A,RPS28,WARS
GO:0006518	peptide metabolic process	7	497	0.0225	EIF2S1,EIF3CL,QARS,RPL36A,RPS28,TAPBP,WARS
GO:0045071	negative regulation of viral genome replication	3	52	0.0225	BST2,ISG15,OAS3
GO:0051639	actin filament network formation	2	10	0.0225	LCP1,PLS1
GO:0051707	response to other organism	9	835	0.0225	BST2,GBP1,IDO1,ISG15,OAS3,PTPRC,PYCARD,SAMHD1,STAT1
GO:0110053	regulation of actin filament organization	5	235	0.0225	CAPG,CAPZA1,CORO1A,PYCARD,WASF2
GO:0002684	positive regulation of immune system process	9	882	0.0258	C1QB,CORO1A,FAM49B,IDO1,ISG15,PTPRC,PYCARD,STAT1,WASF2
GO:0006413	translational initiation	4	142	0.0258	EIF2S1,EIF3CL,RPL36A,RPS28
GO:0030833	regulation of actin filament polymerization	4	141	0.0258	CAPG,CAPZA1,CORO1A,PYCARD
GO:0048514	blood vessel morphogenesis	6	381	0.0258	COL15A1,LRP1,MCAM,TYMP,WARS,WASF2
GO:0051764	actin crosslink formation	2	12	0.0258	LCP1,PLS1
GO:0065007	biological regulation	44	11740	0.0258	BST2,BUB3,C1QB,CAPG,CAPZA1,CBX3,CD2AP,CDYL,COL15A1,CORO1A,EFEMP1,EIF2S1,FAM49B,GBP1,GLG1,HSPB8,IDO1,ISG15,LANCL1,LCP1,LRP1,MCAM,NSFL1C,NT5E,OAS3,PCNA,PLS1,PROS1,PSMC1,PTPRC,PYCARD,QARS,RPL36A,RPS28,S100A4,SAMHD1,SFXN3,SNX1,STAT1,TAPBP,TNC,TYMP,WARS,WASF2
GO:0051241	negative regulation of multicellular organismal process	10	1098	0.0270	BST2,CD2AP,EFEMP1,GBP1,IDO1,ISG15,LRP1,PROS1,PYCARD,STAT1
GO:0042129	regulation of T cell proliferation	4	151	0.0296	CORO1A,IDO1,PTPRC,PYCARD
GO:0051016	barbed-end actin filament capping	2	14	0.0296	CAPG,CAPZA1
GO:0048583	regulation of response to stimulus	21	3882	0.0324	BST2,C1QB,CD2AP,EFEMP1,FAM49B,GBP1,GLG1,HSPB8,IDO1,LRP1,NT5E,PCNA,PROS1,PTPRC,PYCARD,QARS,S100A4,SAMHD1,STAT1,TYMP,WASF2
GO:0060333	interferon-gamma-mediated signaling pathway	3	69	0.0331	GBP1,OAS3,STAT1
GO:0019538	protein metabolic process	22	4194	0.0338	BUB3,C1QB,CD2AP,CPA4,EFEMP1,EIF2S1,EIF3CL,ISG15,LAP3,LRP1,NSFL1C,PCNA,PSMC1,PTPRC,PYCARD,QARS,RPL36A,RPS28,TNC,VCAN,VWA1,WARS
GO:0051128	regulation of cellular component organization	15	2306	0.0338	BST2,BUB3,CAPG,CAPZA1,CD2AP,CORO1A,GBP1,LCP1,LRP1,NSFL1C,PLS1,PSMC1,PYCARD,WARS,WASF2
GO:1903037	regulation of leukocyte cell-cell adhesion	5	278	0.0338	CORO1A,FAM49B,IDO1,PTPRC,PYCARD

GO-term: Gene Ontology terminology.

Supplemental Table S3. Top-50 biological processes (GO terminology) from the 28 significantly under-represented proteins of antibody-mediated glomerular injuries compared to stable graft controls, according to the online resource STRING v11.0, in ascending order of false discovery rate

GO-term	Term description	Observed protein count	Background protein count	False discovery rate	Involved proteins (labels)
GO:0006520	cellular amino acid metabolic process	9	308	3.29e-07	ACADSB,ACAT1,ALDH4A1,ALDH6A1,BHMT,DDC,GATM,GLYAT,SHMT1
GO:0019752	carboxylic acid metabolic process	11	854	5.77e-06	ACADSB,ACAT1,ALDH4A1,ALDH6A1,BHMT,DCXR,DDC,GATM,GLYAT,SHMT1,SORD
GO:1901605	alpha-amino acid metabolic process	7	209	5.77e-06	ACAT1,ALDH4A1,ALDH6A1,BHMT,GATM,GLYAT,SHMT1
GO:0046395	carboxylic acid catabolic process	7	237	7.92e-06	ACADSB,ACAT1,ALDH4A1,ALDH6A1,DCXR,SHMT1,SORD
GO:0044281	small molecule metabolic process	13	1779	3.47e-05	ACADSB,ACAT1,ALDH4A1,ALDH6A1,BHMT,CAT,DCXR,DDC,GATM,GLYAT,PCK2,SHMT1,SORD
GO:0009056	catabolic process	13	1859	5.13e-05	ACADSB,ACAT1,ALDH4A1,ALDH6A1,ANPEP,BHMT,CAT,DCXR,FABP1,GGACT,GPX3,SHMT1,SORD
GO:0009063	cellular amino acid catabolic process	5	114	6.14e-05	ACADSB,ACAT1,ALDH4A1,ALDH6A1,SHMT1
GO:0044248	cellular catabolic process	12	1646	8.82e-05	ACADSB,ACAT1,ALDH4A1,ALDH6A1,ANPEP,BHMT,CAT,DCXR,FABP1,GPX3,SHMT1,SORD
GO:0017144	drug metabolic process	8	622	0.00014	ACAT1,BHMT,CAT,DDC,GATM,GLYAT,GPX3,SHMT1
GO:0009083	branched-chain amino acid catabolic process	3	18	0.00022	ACADSB,ACAT1,ALDH6A1
GO:0051186	cofactor metabolic process	7	467	0.00022	ACAT1,CAT,DCXR,GLYAT,GPX3,GSTA2,SHMT1
GO:0009081	branched-chain amino acid metabolic process	3	21	0.00030	ACADSB,ACAT1,ALDH6A1
GO:0051289	protein homotetramerization	4	78	0.00030	CAT,DCXR,GPX3,SHMT1
GO:0006575	cellular modified amino acid metabolic process	5	185	0.00034	ALDH4A1,BHMT,GATM,GSTA2,SHMT1
GO:1901575	organic substance catabolic process	11	1609	0.00034	ACADSB,ACAT1,ALDH4A1,ALDH6A1,ANPEP,BHMT,DCXR,FABP1,GGACT,SHMT1,SORD
GO:0042133	neurotransmitter metabolic process	4	87	0.00038	BHMT,DDC,GLYAT,SHMT1
GO:0042219	cellular modified amino acid catabolic process	3	28	0.00050	ALDH4A1,BHMT,GGACT
GO:1901606	alpha-amino acid catabolic process	4	98	0.00054	ACAT1,ALDH4A1,ALDH6A1,SHMT1
GO:0055114	oxidation-reduction process	8	923	0.0013	ACADSB,ACAT1,ALDH4A1,ALDH6A1,CAT,DCXR,GPX3,SORD
GO:0019640	glucuronate catabolic process to xylulose 5-phosphate	2	5	0.0016	DCXR,SORD
GO:0032787	monocarboxylic acid metabolic process	6	477	0.0016	ACADSB,ACAT1,ALDH4A1,DCXR,GLYAT,SORD
GO:0051167	xylulose 5-phosphate metabolic process	2	5	0.0016	DCXR,SORD
GO:1901565	organonitrogen compound catabolic process	8	958	0.0016	ACADSB,ACAT1,ALDH4A1,ALDH6A1,ANPEP,BHMT,GGACT,SHMT1
GO:0051187	cofactor catabolic process	3	52	0.0020	ACAT1,CAT,GPX3
GO:0051260	protein homooligomerization	5	312	0.0023	ACAT1,CAT,DCXR,GPX3,SHMT1
GO:1901607	alpha-amino acid biosynthetic process	3	60	0.0027	BHMT,GATM,SHMT1
GO:0044283	small molecule biosynthetic process	6	569	0.0037	ACAT1,BHMT,GATM,PCK2,SHMT1,SORD
GO:0008652	cellular amino acid biosynthetic process	3	77	0.0052	BHMT,GATM,SHMT1
GO:0098869	cellular oxidant detoxification	3	86	0.0070	CAT,FABP1,GPX3
GO:0006544	glycine metabolic process	2	16	0.0074	GLYAT,SHMT1
GO:0006577	amino-acid betaine metabolic process	2	17	0.0078	BHMT,SHMT1
GO:0042744	hydrogen peroxide catabolic process	2	20	0.0100	CAT,GPX3
GO:0009636	response to toxic substance	5	468	0.0109	CAT,DDC,FABP1,GLYAT,GPX3
GO:0072329	monocarboxylic acid catabolic process	3	106	0.0109	ACAT1,DCXR,SORD
GO:0006006	glucose metabolic process	3	113	0.0124	DCXR,PCK2,SORD
GO:0042737	drug catabolic process	3	113	0.0124	ACAT1,CAT,GPX3
GO:0019585	glucuronate metabolic process	2	24	0.0125	DCXR,SORD
GO:1901564	organonitrogen compound metabolic process	16	5281	0.0143	ACADSB,ACAT1,ALDH4A1,ALDH6A1,ANPEP,BHMT,CAT,CR1,DCXR,DDC,

					GATM,GGACT,GLYAT,GSTA2,SHMT1,TINAG
GO:0006732	coenzyme metabolic process	4	297	0.0151	ACAT1,DCXR,GLYAT,SHMT1
GO:0042743	hydrogen peroxide metabolic process	2	31	0.0179	CAT,GPX3
GO:0008152	metabolic process	22	9569	0.0225	ACADSB,ACAT1,ALDH4A1,ALDH6A1,ANPEP,BHMT,CAT,CMBL,CR1,DCXR,DDC,FABP1,GATM,GGACT,GLYAT,GPX3,GSTA2,PBLD,PCK2,SHMT1,SORD,TINAG
GO:0006790	sulfur compound metabolic process	4	343	0.0241	ACAT1,BHMT,GLYAT,GSTA2
GO:0009112	nucleobase metabolic process	2	38	0.0244	ALDH6A1,SHMT1
GO:0042398	cellular modified amino acid biosynthetic process	2	41	0.0272	GATM,SHMT1
GO:0042136	neurotransmitter biosynthetic process	2	42	0.0280	DDC,SHMT1
GO:0044272	sulfur compound biosynthetic process	3	172	0.0294	ACAT1,BHMT,GSTA2
GO:0097164	ammonium ion metabolic process	3	179	0.0323	BHMT,DDC,SHMT1
GO:0055086	nucleobase-containing small molecule metabolic process	5	662	0.0337	ACAT1,ALDH6A1,DCXR,GLYAT,SHMT1
GO:0019319	hexose biosynthetic process	2	49	0.0346	PCK2,SORD
GO:0006576	cellular biogenic amine metabolic process	2	50	0.0354	BHMT,DDC

GO-term: Gene Ontology terminology.

Supplemental Table S4. Interpretation results of the WARS antibody by immunohistochemistry in the diagnosis of active antibody-mediated rejection in the independent biopsy cohort

	WARS positivity for active ABMR according to pathologist 1		WARS positivity for active ABMR according to pathologist 2	
Diagnosis	**Number of total cases (n=53)**	**Number of cases considered positive, n (%)**	**Number of total cases (n=53)**	**Number of cases considered positive, n (%)**
Active ABMR	16	12 (75)	16	11 (69)
Non active cABMR	5	2 (40)	5	2 (40)
Isolated C4d	3	1 (33)	3	1 (33)
SG ABO incompatible	3	0 (0)	3	0 (0)
Non humoral TMA	5	0 (0)	5	0 (0)
Acute TCMR	6	1 (17)	6	0 (0)
Infection (PVN, APN)	5	1 (20)	5	1 (20)
ATI	5	0 (0)	5	1 (20)
Recurrent GN	5	0 (0)	5	1 (20)

Each pathologist, 1 (BC) and 2 (AV), interpreted the WARS staining, by focusing on the endothelial cells, and blindly classified them as positive or negative for active ABMR. WARS positivity requires a strong and diffuse endothelial staining in at least one microcirculation compartment (either glomeruli and/or peritubular capillaries). Peritubular capillaries staining should not be assessed in areas of marked tubulo-interstitial inflammation. Pathologists were formerly trained for interpretation with the slides set from the spectrometric cohort. SG ABO incompatible cases refer to one year protocol biopsies in an ABO incompatible transplantation without significant inflammation. Abbreviations: ABMR, antibody-mediated rejection; WARS, tryptophan--tRNA ligase, cytoplasmic; cABMR, chronic antibody-mediated rejection; SG, stable graft, TMA, thrombotic microangiopathy; TCMR, T-cell mediated rejection; PVN, polyomavirus nephropathy; APN, acute pyelonephritis; ATI, acute tubular injuries; GN, glomerulonephritis.

Supplemental Table S5. Diagnostic performances of the WARS antibody in the diagnosis of active antibody-mediated rejection by immunohistochemistry, according to pathologists 1 and 2

	Pathologist 1 (BC)		Pathologist 2 (AV)		
	WARS interpreted as positive for active ABMR	**WARS interpreted as negative for active ABMR**	**WARS interpreted as positive for active ABMR**	**WARS interpreted as negative for active ABMR**	**Total, n (%)**
Active ABMR	12	4	11	5	16 (30)
Everything else	5	32	6	31	37 (70)
Total, n (%)	17 (32)	36 (68)	17 (32)	36 (68)	53 (100)

Everything else refers to all included differential diagnoses in the cohort, as detailed in Table 5, including chronic antibody-mediated rejections without histological activity, non-humoral thrombotic microangiopathies, one year protocol ABO incompatible biopsies, T-cell mediated rejections, polyomavirus nephropathies, acute pyelonephritides, acute tubular injuries and recurrent glomerulonephritides. Abbreviations: ABMR, antibody-mediated rejection; WARS, tryptophan--tRNA ligase, cytoplasmic.

Supplemental Table S6. Interpretation results of the TYMP antibody by immunohistochemistry in the diagnosis of active antibody-mediated rejection in the independent biopsy cohort

	TYMP positivity for active ABMR according to pathologist 1		TYMP positivity for active ABMR according to pathologist 2	
Diagnosis	**Number of total cases (n=52)**	**Number of cases considered positive (n,%)**	**Number of total cases (n=52)**	**Number of cases considered positive (n,%)**
Active ABMR	16	14 (88)	16	12 (75)
Non active cABMR	5	2 (40)	5	2 (40)
Isolated C4d	3	1 (33)	3	1 (33)
SG ABO incompatible	3	0 (0)	3	0 (0)
Non humoral TMA	5	0 (0)	5	0 (0)
Acute TCMR	6	2 (33)	6	0 (0)
Infection (PVN, APN)	4	0 (0)	4	0 (0)
ATI	5	0 (0)	5	0 (0)
Recurrent GN	5	0 (0)	5	1 (20)

Each pathologist, 1 (BC) and 2 (AV), interpreted the TYMP staining, by focusing on the endothelial cells, and blindly classified them as positive or negative for active ABMR. TYMP positivity requires a strong and diffuse endothelial staining in at least one microcirculation compartment (either glomeruli and/or peritubular capillaries). Peritubular capillaries staining should not be assessed in areas of marked tubulo-interstitial inflammation. Pathologists were formerly trained for interpretation with the slides set from the spectrometric cohort. SG ABO incompatible cases refer to one year protocol biopsies in an ABO incompatible transplantation without significant inflammation. Abbreviations: ABMR, antibody-mediated rejection; TYMP, thymidine phosphorylase; cABMR, chronic antibody-mediated rejection; SG, stable graft, TMA, thrombotic microangiopathy; TCMR, T-cell mediated rejection; PVN, polyomavirus nephropathy; APN, acute pyelonephritis; ATI, acute tubular injuries; GN, glomerulonephritis.

Supplemental Table S7. Diagnostic performances of the TYMP antibody in the diagnosis of active antibody-mediated rejection by immunohistochemistry, according to pathologists 1 and 2

	Pathologist 1 (BC)		Pathologist 2 (AV)		
	TYMP interpreted as positive for active ABMR	**TYMP interpreted as negative for active ABMR**	**TYMP interpreted as positive for active ABMR**	**TYMP interpreted as negative for active ABMR**	Total, n (%)
Active ABMR	14	2	12	4	16 (31)
Everything else	5	31	4	32	36 (69)
Total, n (%)	19 (37)	33 (63)	16 (31)	36 (69)	52 (100)

Everything else refers to all included differential diagnoses in the cohort, as detailed in Table 5, including chronic antibody-mediated rejections without histological activity, non-humoral thrombotic microangiopathies, one year protocol ABO incompatible biopsies, T-cell mediated rejections, polyomavirus nephropathies, acute pyelonephritides, acute tubular injuries and recurrent glomerulonephritides. Abbreviations: ABMR, antibody-mediated rejection; TYMP, thymidine phosphorylase.

Supplemental Table S8. Interpretation results of the GBP1 antibody by immunohistochemistry in the diagnosis of active antibody-mediated rejection in the independent biopsy cohort

	GBP1 positivity for active ABMR according to pathologist 1		GBP1 positivity for active ABMR according to pathologist 2	
Diagnosis	**Number of total cases (n=52)**	**Number of cases considered positive (n,%)**	**Number of total cases (n=52)**	**Number of cases considered positive (n,%)**
Active ABMR	15	9 (60)	15	10 (67)
Non active cABMR	5	2 (40)	5	1 (20)
Isolated C4d	3	1 (33)	3	1 (33)
SG ABO incompatible	3	0 (0)	3	0 (0)
Non humoral TMA	5	0 (0)	5	0 (0)
Acute TCMR	6	1 (17)	6	0 (0)
Infection (PVN, APN)	5	1 (20)	5	0 (0)
ATI	5	0 (0)	5	1 (20)
Recurrent GN	5	0 (0)	5	1 (20)

Each pathologist, 1 (BC) and 2 (AV), interpreted the GBP1 staining, by focusing on the endothelial cells, and blindly classified them as positive or negative for active ABMR. GBP1 positivity was considered when at least a third of a microcirculation compartment (glomeruli and/or peritubular capillaries) was strongly stained, even if segmental. Peritubular capillaries staining should not be assessed in areas of marked tubulo-interstitial inflammation. Pathologists were formerly trained for interpretation with the slides set from the spectrometric cohort. SG ABO incompatible cases refer to one year protocol biopsies in an ABO incompatible transplantation without significant inflammation. Abbreviations: ABMR, antibody-mediated rejection; GBP1, guanylate-binding protein 1; cABMR, chronic antibody-mediated rejection; SG, stable graft, TMA, thrombotic microangiopathy; TCMR, T-cell mediated rejection; PVN, polyomavirus nephropathy; APN, acute pyelonephritis; ATI, acute tubular injuries; GN, glomerulonephritis.

Supplemental Table S9. Diagnostic performances of the GBP1 antibody in the diagnosis of active antibody-mediated rejection by immunohistochemistry, according to pathologists 1 and 2

	Pathologist 1 (BC)		Pathologist 2 (AV)		
	GBP1 interpreted as positive for active ABMR	**GBP1 interpreted as negative active ABMR**	**GBP1 interpreted as positive for active ABMR**	**GBP1 interpreted as negative active ABMR**	Total, n (%)
Active ABMR	9	6	10	5	15 (29)
Everything else	5	32	4	33	37 (71)
Total, n (%)	14 (27)	38 (73)	14 (27)	38 (73)	52 (100)

Everything else refers to all included differential diagnoses in the cohort, as detailed in supplemental Table S6 and the Methods section, including chronic antibody-mediated rejections without histological activity, non-humoral thrombotic microangiopathies, one year protocol ABO incompatible biopsies, T-cell mediated rejections, polyomavirus nephropathies, acute pyelonephritides, acute tubular injuries and recurrent glomerulonephritides. Abbreviations: ABMR, antibody-mediated rejection; GBP1, guanylate-binding protein 1.

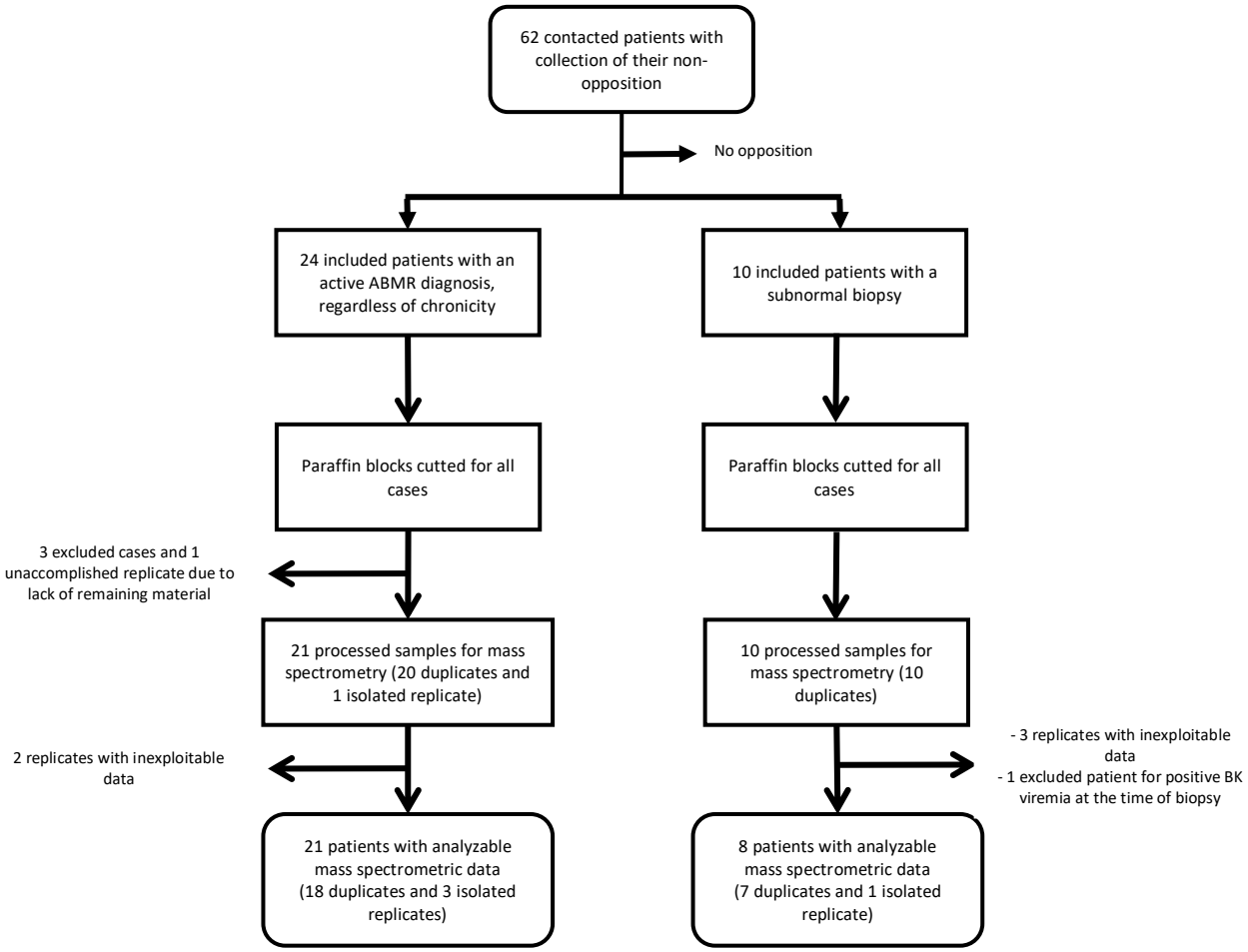

Supplemental Figure S1. Flow-chart of the GlomProt study. Active antibody-mediated rejection (aABMR) cases were consistent with the Banff 2017 classification, but also all cases included in this group had anti-HLA donor-specific antibodies at the time of diagnosis and had a positive glomerulitis score (g>0). The inexploitable spectrometric data were due to overpressures in the pre-column of chromatography for some samples during processing, of unknown cause, which led to a misalignment of the spectrometric profiles and/or to poor protein identification performances.

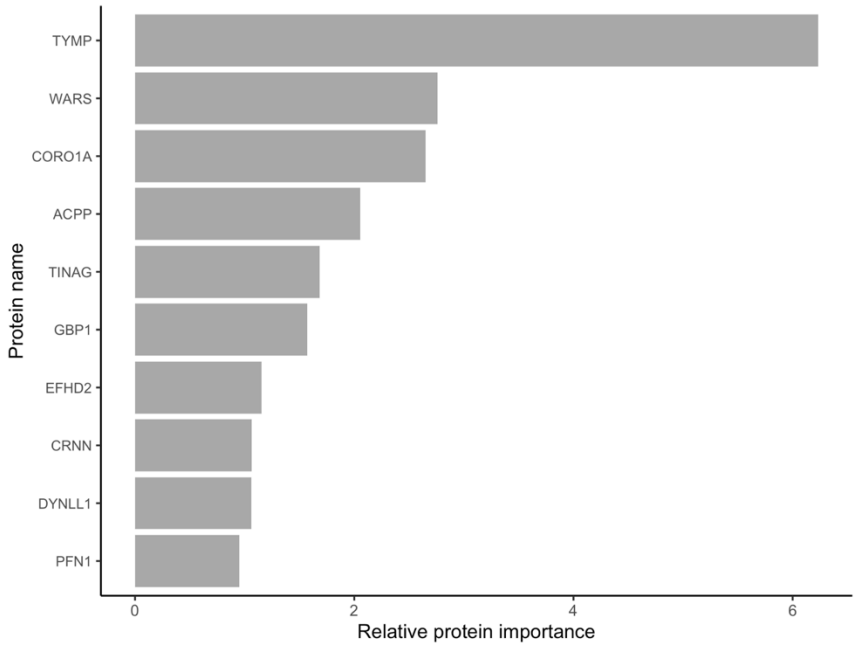

Supplemental Figure S2. Random forest analysis showing the relative importance of proteins abundance to classify the samples as antibody-mediated rejection or stable graft. X-axis shows the relative importance of each variable. The selected model was composed of 10 different variables/proteins. Error rate is 0%. All samples were analyzed.

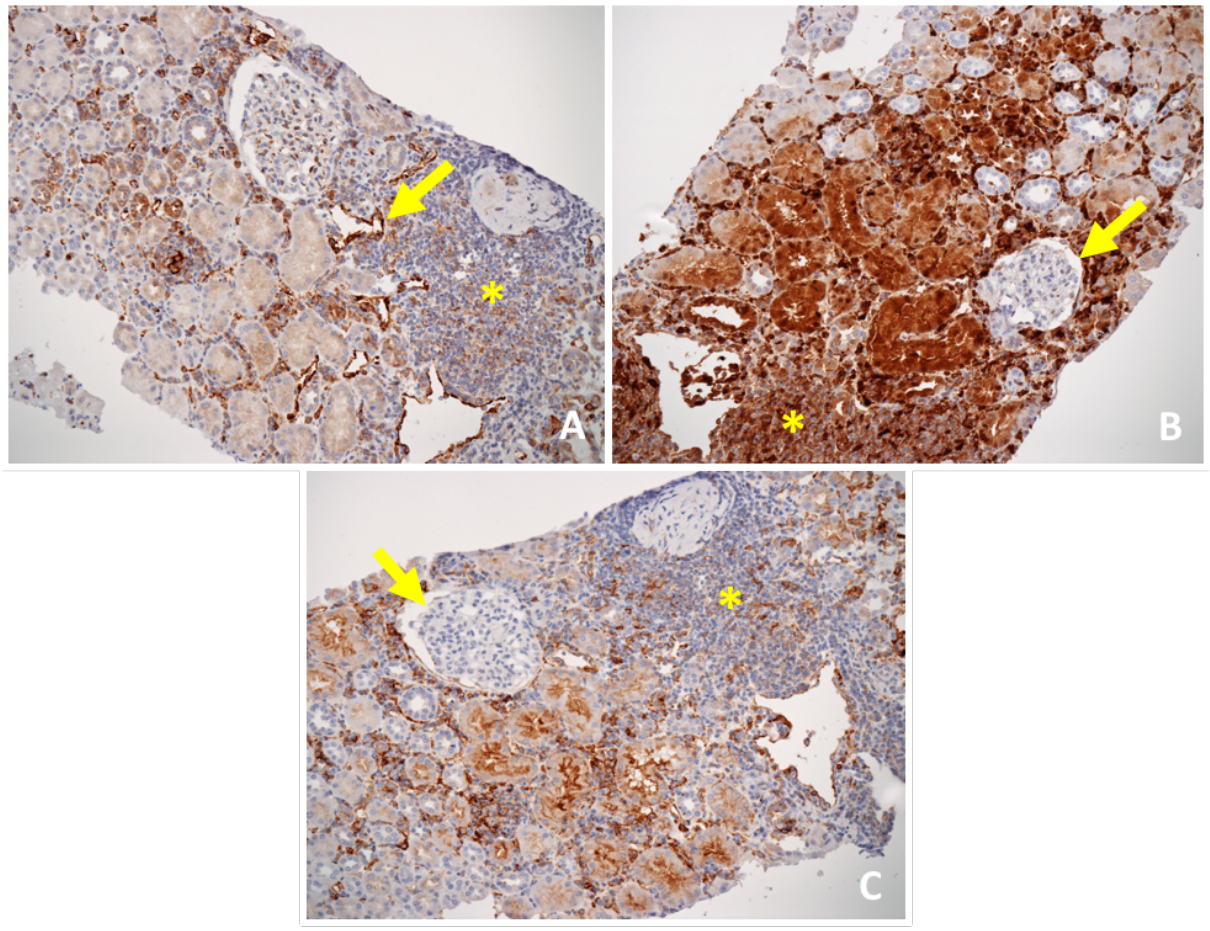

Supplemental Figure S3. Immunohistochemical stainings for WARS, TYMP and GBP1 in a T-cell mediated rejection, original magnification x100. (A) WARS staining. Note the strong endothelial positivity (arrow) nearby the inflammatory infiltrate (asterisk) in peritubular capillaries on the right-hand side, which should not be considered as an active humoral process. Endothelial positivity in the glomerulus in weak, similar to constitutive staining. We could also notice a sparse weak positivity of the inflammatory cells and of some tubular cells. (B) TYMP staining. Note that, while there is a strong tubulo-interstitial positivity (asterisk), including tubular, inflammatory and endothelial cells, where the staining should not be considered as an active humoral process, the glomerulus is strictly negative (arrow). (C) GBP1 staining. A sparse moderate staining of endothelial and inflammatory cells is seen (asterisk), while the permeable glomerulus is negative (arrow). Positive proximal tubular cells are seen nearby the inflammatory infiltrate, predominant in the brush border.

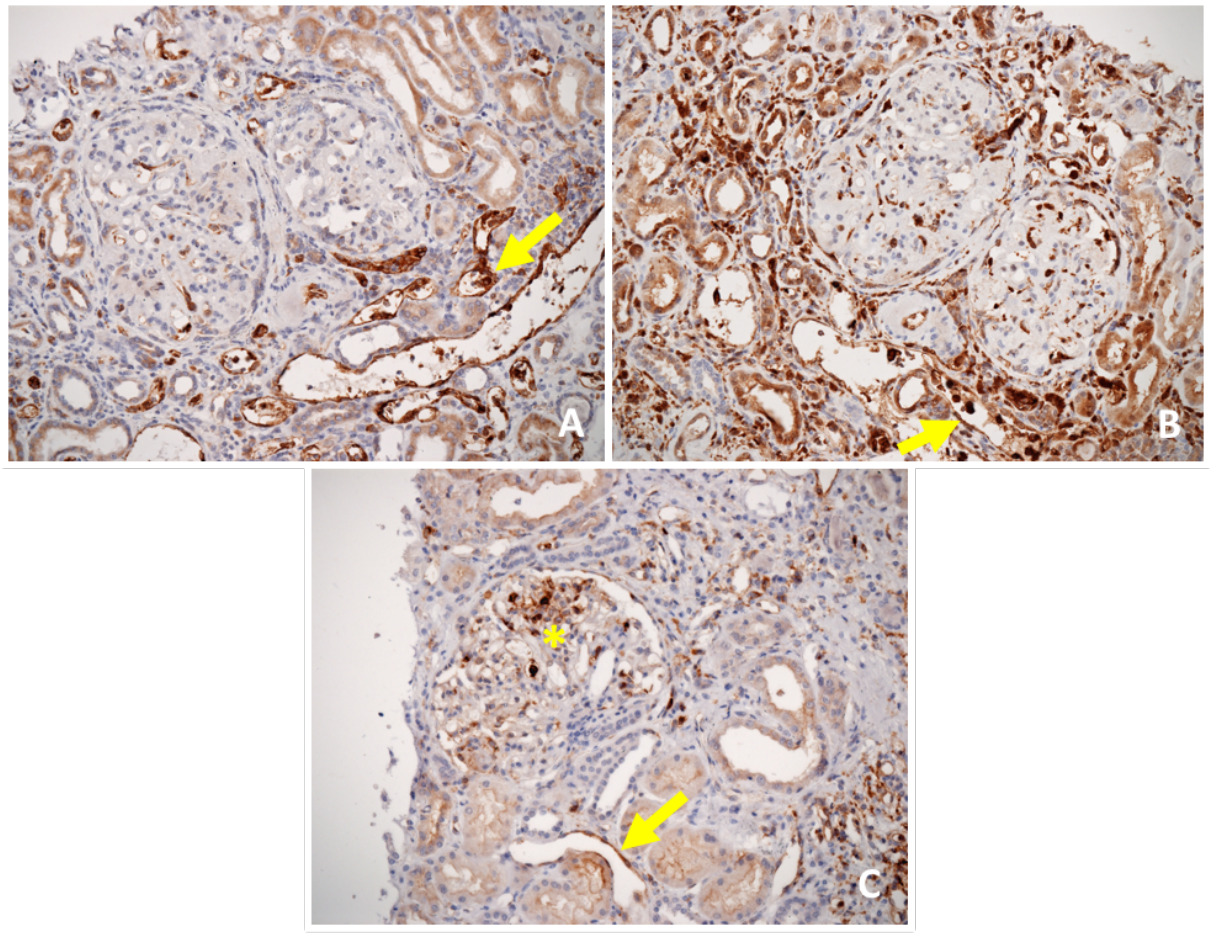

Supplemental Figure S4. Immunohistochemical stainings for WARS, TYMP and GBP1 in a chronic antibody-mediated rejection case, without activity according to the 2017 Banff classification, especially with no microvascular inflammation (g0 cpt0), original magnification x200. (A) WARS staining. Note the strong endothelial positivity on peritubular capillaries (arrow), that prompted the pathologist to a misclassification as active antibody-mediated rejection (ABMR). Positivity of the glomeruli is sparse, itself insufficient to retain a diagnosis of ABMR. A weak and diffuse positivity is observed in tubular cells. (B) TYMP staining. A strong positivity is seen in inflammatory cells as well as a moderate expression in tubular cells, that makes it difficult to assess endothelial positivity, which is moderate in peritubular capillaries (arrow) and weak in the glomeruli. This case was misclassified by one of the pathologist. (C) GBP1 staining. A globally moderate segmental staining is visible in the glomerulus (asterisk), on some endothelial and inflammatory cells. In the peritubular capillaries, a moderate and sparse staining is seen on some endothelial cells (arrow). This case was misclassified by one of the pathologist.

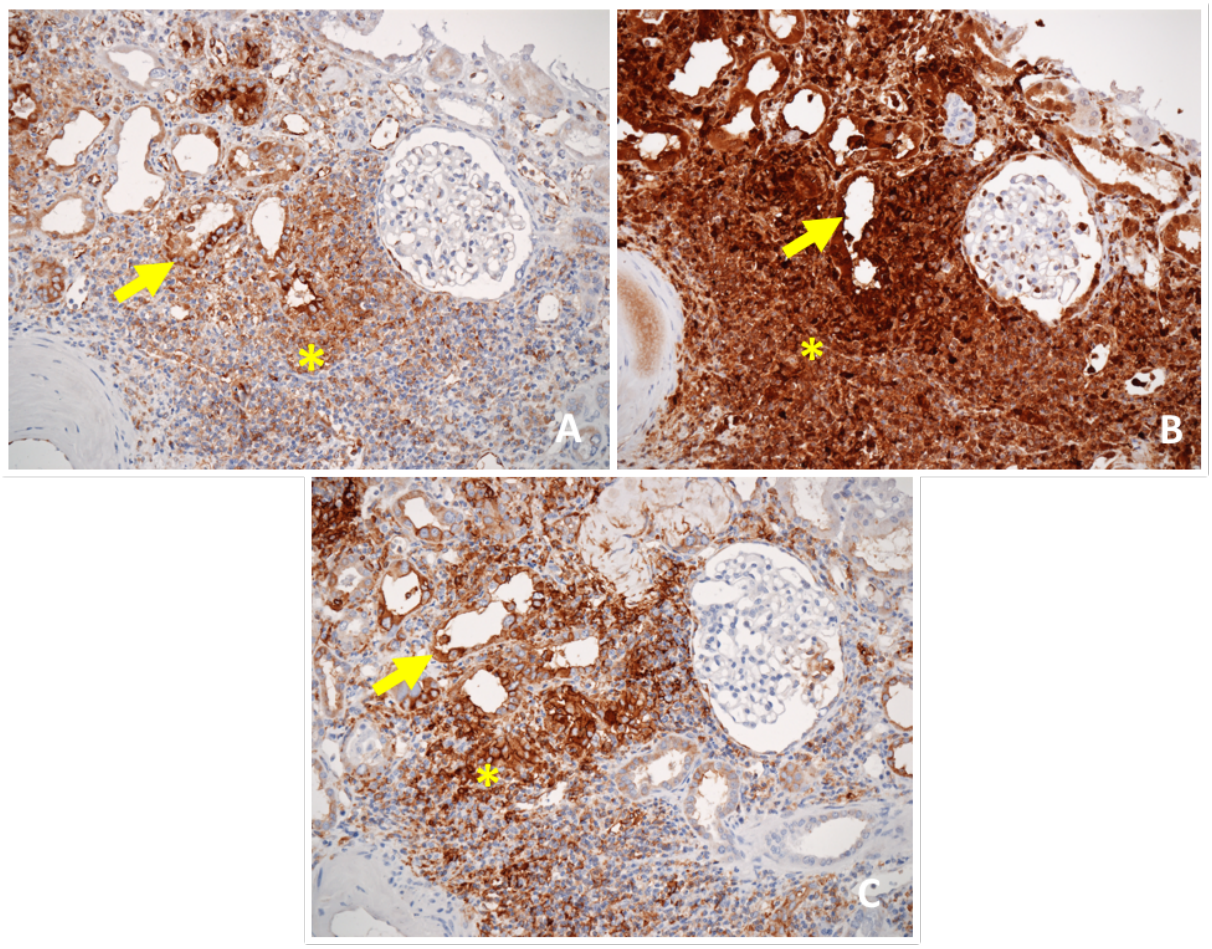

Supplemental Figure S5. Immunohistochemical stainings for WARS, TYMP and GBP1 in a polyomavirus nephropathy, original magnification x100. (A) WARS staining. Note the highly inflammatory tubulo-interstitial compartment, where a moderate staining is observed in some inflammatory cells (asterisk) and a strong expression is seen in tubular cells (arrow), with marked tubulopathy features. Endothelial staining in peritubular capillaries should not be considered in this area for an ABMR diagnosis. The glomerulus is negative, that prompted the pathologists to classify against a humoral process. (B) TYMP staining. Note that, while there is a strong tubulo-interstitial positivity, including tubular (arrow), inflammatory (asterisk) and probably endothelial cells, where the staining should not be considered for an ABMR diagnosis, a weak expression is seen on sparse cells in the glomerulus. (C) GBP1 staining. A moderate to strong staining of inflammatory (asterisk) and tubular cells (arrow) is seen, while endothelial expression is difficult to assess in peritubular capillaries. The glomerulus only shows a weak and segmental expression, the others being negative (elsewhere in the biopsy).

Serment d'Hippocrate

Au moment d'être admis à exercer la médecine, je promets et je jure d'être fidèle aux lois de l'honneur et de la probité.

Mon premier souci sera de rétablir, de préserver ou de promouvoir la santé dans tous ses éléments, physiques et mentaux, individuels et sociaux.

Je respecterai toutes les personnes, leur autonomie et leur volonté, sans aucune discrimination selon leur état ou leurs convictions. J'interviendrai pour les protéger si elles sont affaiblies, vulnérables ou menacées dans leur intégrité ou leur dignité. Même sous la contrainte, je ne ferai pas usage de mes connaissances contre les lois de l'humanité.

J'informerai les patients des décisions envisagées, de leurs raisons et de leurs conséquences.

Je ne tromperai jamais leur confiance et n'exploiterai pas le pouvoir hérité des circonstances pour forcer leurs consciences.

Je donnerai mes soins à l'indigent et à quiconque me les demandera. Je ne me laisserai pas influencer par la soif du gain ou la recherche de la gloire.

Admis dans l'intimité des personnes, je tairai les secrets qui me seront confiés. Reçu à l'intérieur des maisons, je respecterai les secrets des foyers et ma conduite ne servira pas à corrompre les mœurs.

Je ferai tout pour soulager les souffrances. Je ne prolongerai pas abusivement les agonies. Je ne provoquerai jamais la mort délibérément.

Je préserverai l'indépendance nécessaire à l'accomplissement de ma mission. Je n'entreprendrai rien qui dépasse mes compétences. Je les entretiendrai et les perfectionnerai pour assurer au mieux les services qui me seront demandés.

J'apporterai mon aide à mes confrères ainsi qu'à leurs familles dans l'adversité.

Que les hommes et mes confrères m'accordent leur estime si je suis fidèle à mes promesses ; que je sois déshonoré et méprisé si j'y manque.

Titre : Identification de nouveaux immunomarqueurs du rejet humoral actif en transplantation rénale à travers l'analyse du protéome glomérulaire par spectrométrie de masse

Résumé :
Contexte : Le diagnostic de rejet humoral actif (RHA) en transplantation rénale humaine reste complexe, car les critères histologiques clés, l'évaluation de l'inflammation de la microcirculation et les dépôts de C4d, manquent encore de reproductibilité et de sensibilité respectivement.
Méthodes : Nous avons analysé, à l'aide du couple microdissection laser et spectrométrie de masse en tandem, les modifications du protéome glomérulaire au cours du RHA par rapport à des contrôles greffés stables (SG) à partir de biopsies fixées en formol et incluses en paraffine (FFPE), et identifié des candidats biomarqueurs diagnostiques du RHA. Ces derniers ont été secondairement évalués en immunohistochimie par deux pathologistes sur une cohorte rétrospective indépendante de 53 cas.
Résultats : 21 cas de RHA et 8 SG ont été analysés. Nous avons défini un profil de 82 protéines impliquées dans les lésions glomérulaires humorales, traduisant une activation leucocytaire, un stress cellulaire médié par les interférons de type I et II et un remodelage de la microcirculation. Nous avons sélectionné trois protéines pour l'étude immunohistochimique : la thymidine phosphorylase (TYMP), la *guanylate-binding protein 1* (GBP1) et la *tryptophan--tRNA ligase, cytoplasmic* (WARS). Les meilleures performances dans le diagnostic de RHA ont été obtenues avec TYMP et WARS, avec respectivement une sensibilité moyenne de 82% et 72%, une spécificité moyenne de 88% et 85%, et une reproductibilité forte ($\kappa = 0,7$) et modérée ($\kappa = 0,567$).
Conclusion : Nous décrivons le premier profil protéique glomérulaire du RHA en transplantation rénale à partir d'échantillons FFPE, marqué par la voie de signalisation des interférons et le remodelage de la microcirculation. Nous mettons en évidence deux marqueurs pertinents à étudier par immunohistochimie, WARS et TYMP, avec de prime abord de bonnes performances dans le diagnostic du RHA, qui doivent maintenant être évaluées sur de plus larges cohortes prospectives.

Mots-clés : rejet humoral, glomérule, protéomique, spectrométrie de masse, transplantation rénale, biomarqueur

Title: Identification of new immunomarkers of active antibody-mediated rejection through glomerular proteome analysis in kidney transplantation

Abstract:
Background: Issues remain in the diagnosis of antibody-mediated rejection (ABMR) in human kidney transplantation, as the hallmark criteria, the microcirculation inflammation scores and C4d deposits, still lack reproducibility and sensitivity respectively.
Methods: We used laser microdissection coupled with tandem mass spectrometry-based proteomics from formalin-fixed and paraffin embedded (FFPE) biopsies to describe the protein profile of antibody-mediated glomerular injuries in human kidney transplantation compared to stable graft controls (SG), and to identify diagnostic biomarkers of active ABMR for daily practice. These latter were secondarily assessed by immunohistochemistry in an independent retrospective cohort of 53 cases by two pathologists.
Results: 21 active ABMR and 8 SG were analyzed. We defined a profile of 82 proteins involved in antibody-mediated glomerular injuries, marked by evidences of leukocyte activation, cellular stress mediated by the type I and II interferons as well as microcirculation remodeling. We selected three interferon-related endothelial stress proteins for immunohistochemistry: thymidine phosphorylase (TYMP), guanylate-binding protein 1 (GBP1) and tryptophan--tRNA ligase, cytoplasmic (WARS). TYMP and WARS had the best performances for the diagnosis of active ABMR, with a mean sensitivity of 82% and 72%, a mean specificity of 88% and 85%, and a substantial (κ=0,7) and moderate (κ=0,567) agreement respectively.
Conclusion: We describe the first glomerular protein profile of ABMR in kidney transplantation from FFPE samples, marked by the interferons environment and microcirculation remodeling. We highlight two relevant immunohistochemical markers, WARS and TYMP, with *prima facie* good performances in the diagnosis of active ABMR, which now need to be assessed in a prospective larger cohort.

Keywords: antibody-mediated rejection, glomerulus, proteomics, mass spectrometry, kidney transplantation, biomarker

Discipline : MEDECINE – ANATOMIE ET CYTOLOGIE PATHOLOGIQUES

UFR des sciences médicales – Université de Bordeaux – 146 rue Léo Saignat 33076 Bordeaux Cedex